Universidade do Minho
Escola de Medicina

João Manuel do Canto Gomes

Impact of the immune system aging on multiple sclerosis' forms of progression: study of the thymic function

junho de 2017

UMinho | 2017 João Gomes **Impact of the immune system aging on multiple sclerosis' forms of progression: study of the thymic function**

Universidade do Minho
Escola de Medicina

João Manuel do Canto Gomes

Impact of the immune system aging on multiple sclerosis' forms of progression: study of the thymic function

Impacto do envelhecimento do sistema imunitário nas diferentes formas de progressão de esclerose múltipla: estudo da função tímica

Dissertação de Mestrado

Mestrado em Ciências da Saúde

Trabalho efetuado sob a orientação da

Doutora Cláudia Nóbrega

e da

Profª Doutora Margarida Correia-Neves

junho 2017

The work presented in this thesis was performed in the Life and Health Sciences Research Institute (ICVS), School of Medicine, University of Minho, ICVS/3B's – PT Government Associate Laboratory, Braga/Guimarães, Portugal. This work was developed under the scope of the project NORTE-01-0246-FEDER-000012, supported by the Northern Portugal Regional Operational Program (NORTE 2020), under the Portugal 2020 Partnership Agreement, through the European Regional Development Fund (FEDER, through the Competitiveness Factors Operational Program (COMPETE), and by National funds, through the Foundation for Science and Technology (FCT), under the scope of the project POCI-01-0145-FEDER-007038.

Cofinanciado por:

COMPETE 2020 PORTUGAL 2020 UNIÃO EUROPEIA Fundo Europeu de Desenvolvimento Regional FCT Fundação para a Ciência e a Tecnologia NORTE2020 PROGRAMA OPERACIONAL REGIONAL DO NORTE

"**The highest result of education is tolerance**"

Helen Keller

Acknowledgements

Quero agradecer à pessoa mais importante e sem a qual nada disto teria sido possivel. Cláudia, obrigado por acreditares em mim, obrigado por não teres sido apenas uma orientadora mas acima de tudo uma amiga. Tenho de agradecer todo o esforço que aplicaste no meu trabalho e por teres estado sempre presente mesmo quando as circunstâncias não o propiciavam. Obrigado por me teres ensinado tanto e por me teres ajudado a crescer tanto. Sinto-me um felizardo por poder contar contigo e por ser teu aluno. Obrigado pelo cuidado e preocupação sempre mostrados. Obrigado por tudo.

Margarida obrigado por teres estado sempre presente. Obrigado por me incentivares e me ensinares a cada dia. Obrigado por me dares ferramentas que certamente farão de mim um melhor investigador. Obrigado por me teres dado a oportunidade de trabalhar contigo e com todos os pupilos MCN. É um previlégio ser um MCN.

Rita foi e é um gosto partilhar a secretária contigo. Obrigado pelos bons momentos, pelas gargalhas e pela prontidão em ajudar sempre que necessário. É um privilégio trabalhar contigo.

Um agradecimento muito especial ao Doutor João Cerqueira. Obrigado por todo o apoio prestado no hospital e com os doentes e por todos os esclarecimentos solicitados.

A todos os MCN e/ou MIRD obrigado por me acolherem e fazer do vosso espaço o nosso espaço. Obrigado pela boa disposição, pelas brincadeiras, pela ajuda e por tornarem a nossa segunda casa um local excepcional para trabalhar. Particularmente Margarida, Inês, Alex, Belém e Catarina obrigado pela vossa boa disposição.

Um agradecimento muito especial às pessoas que me previlegiaram a sua amizade e muito em particular Mariana, Boas, Samanta, Magda, Sofia, Rita, Lau, Steph, Marisa, e Sónia. Não poderia pedir melhores amigas.

Obrigado Paulinho, Ricardo, Amorim, Bruno e Miguel por fazerem a minha vida muito mais animada e descontraida. Obrigado por serem os piores e os melhores amigos do mundo. Muito obrigado pela vossa amizade incondicional.

Obrigado a todos os meus amigos.

Um agradecimento particular à associação Todos pela Esclerose Múltipla (TEM), ao Centro Clinico Académico (2CA), ao Hospital de braga, em particular ao enfermeiro Ribeiro e restantes enfermeiros do hospital de dia, e a todos os doentes que aceitaram entrar neste estudo.

Um agradecimento acrescido à professora doutora Paula Ludovico pelo seu papel enquanto diretora do mestrado. Obrigado pelos esclarecimentos e pela disponibilidade sempre mostrados.

Um agradecimento muito especial aos meus pais, aos meus avós, ao meu irmão e à Ana por todo o apoio e carinho sempre mostrados. Obrigado por serem a melhor familia do mundo. Obrigado por me apoiarem sempre. Obrigado por me aconselharem a seguir sempre os meus sonhos e por estarem do meu lado independentemente das minhas escolhas. Obrigado pelos vossos conselhos e pelo vosso esforço em fazer de mim alguem muito feliz. E acima de tudo muito obrigado pela vossa paciência.

Abstract

Multiple sclerosis (MS) is an autoimmune disease from the central nervous system (CNS) characterized by progressive demyelination of neurons. It is a very heterogeneous disease with three main forms of progression: the relapsing-remitting MS, the primary progressive MS and the secondary progressive MS. The lesions in the CNS constitute the hallmark of the disease and are associated with an autoimmune response. In MS, the immune response has been attributed to myelin-autoreactive T lymphocytes. T lymphocytes are produced in the thymus, an immune system primary organ that is very active during the first year of life and involutes progressively with age. Thymic involution contributes to the aging process of the immune system, refered as immunosenescence. Existing data suggest that individuals with RRMS have decreased thymic function when compared to age-matched healthy individuals. The main objective of this study is to investigate how thymic function and immune system aging correlate with the different forms of progression of MS. We hypothesize that the thymic function and the immune system aging may have an essential role for the pathophysiology and progression of the disease. To address this hypothesis, blood samples from MS patients with different forms of disease progression and from healthy individuals were analyzed. Thymic function and immune system aging were then evaluated through quantification of recent thymic emigrants (RTEs) and quantification of the naïve to memory T lymphocytes' ratio, respectively. Our results suggest that the percentage of RTEs and the naïve to memory T lymphocytes' ratio correlate to individual's age similarly on healthy *vs.* MS treatment-naïve individuals. Interestingly, MS individuals on treatment seem to present an increased accumulation of memory subsets in the periphery and decreased thymic function. Altogether, our results suggest that alterations on thymic function and T lymphocytes subsets reported in previous studies are characteristic of MS patients on treatment but not of naïve-treatment individuals. To support our conclusion it is essential, however, to evaluate other surrogates of thymic function (*e.g.* T cell receptor excision circles [TRECs]) and of immunosenescence (*e.g.* relative length of telomere repeats) and extend this study to an increased number of MS patients. So far, we could optimize the flow-FISH technique to quantify the length of telomere repeats on T lymphocytes, introducing several modifications to the protocol previously described by others. Furthermore, although not yet optimized we could verify some progresses on the optimization of the Nested-PCR to TRECs quantification.

Resumo

A esclerose múltipla (EM) é uma doença autoimune do sistema nervoso central (SNC) caracterizada pela desmielinização progressiva dos neurónios. Trata-se de uma doença muito heterogénea com três formas principais de progressão: a forma de surto-remissão, a forma primária progressiva e a forma secundária progressiva. Com o tempo, os efeitos cumulativos da doença juntamente com a falta de tratamentos eficazes levam a défices motores, cognitivos e emocionais. A doença carateriza-se pela ocorrência de lesões no SNC resultantes de uma resposta auto-imune. Na EM, a inflamação tem sido atribuída à existência de linfócitos T auto-reactivos para a mielina. Os linfócitos T são produzidos pelo timo, um órgão primário do sistema imunitário muito ativo nos primeiros anos de vida e que involui de forma progressiva com a idade. A involução do timo contribui para o processo de envelhecimento do sistema imunitário, referido como imunosenescência. Os dados existentes sugerem que indivíduos com forma de surto-remissão possuem menor função tímica quando comparados com indivíduos saudáveis com a mesma idade. O principal objetivo deste estudo é investigar de que forma a função tímica e o envelhecimento do sistema imunitário se correlacionam com a manifestação das diferentes formas de progressão da doença. Colocamos a hipótese de que a função tímica e o envelhecimento do sistema imunitário poderão ter um papel essencial para a patofisiologia e progressão da EM. Para investigar esta hipótese foram analisadas amostras de sangue de indivíduos saudáveis ou doentes com diferentes formas de progressão de EM. A função tímica assim como o envelhecimento do sistema imunitário foram posteriormente avaliados através da quantificação de células recentemente exportadas do timo e da quantificação do rácio de linfócitos T naive sobre linfócitos T de memória, respetivamente. Os nossos resultados sugerem que a percentagem de células recentemente exportadas do tímo e o rácio naive/memória dos linfócitos T se correlacionam com a idade dos indivíduos de forma semelhante em indivíduos saudáveis e com EM sem tratamento. Curiosamente, indivíduos com EM e em tratamento parecem apresentar uma maior acumulação das subpopulações de memória na periferia e diminuição da função tímica. Sucintamente, os nossos resultados sugerem que as alterações na função tímica e nas subpopulações de linfócitos T reportadas em estudos anteriores são características de doentes com EM em tratamento mas não de individuos sem tratamento. Para sustentar os nossos resultados é essencial, no entanto, avaliar outros parâmetros para a função tímica (por exemplo os círculos de excisão do recetor das células T [CERT]) e para a imunosenescência (por exemplo o tamanho relativo dos telómeros) e

alargar este estudo a um maior número de doentes com EM. Até ao momento fomos capazes de otimizar o flow-FISH para a quantificação do tamanho das repetições teloméricas em linfócitos T, introduzindo várias modificações ao protocolo previamente descrito por outros. Não obstante, apesar de ainda não otimizada fomos capazes de fazer progressos na otimização do Nested-PCR para a quantificação de CERTs.

TABLE OF CONTENTS

Abbreviation List

BBB	Blood Brain Barrier
CAM	Cell Adhesion Molecule
CCL	Chemokine Ligand
CCR	C-C Chemokine Receptor
CD	Cluster of Differentiation
CIS	Clinical Isolated Syndrome
CM	Central Memory
CNS	Central Nervous System
CSF	Cerebrospinal Fluid
CXCR	C-X-C Chemokine Receptor
DMSO	Dimethyl Sulfoxide
DN	Double Negative
DNA	Deoxyribonucleic Acid
DP	Double Positive
EAE	Experimental Autoimmune Encephalomyelitis
EDSS	Expanded Disability Status Scale
EM	Effector Memory
FBS	Foetal Bovine Serum
FISH	Fluorescence *in situ* Hybridization
HLA	Human Leukocyte Antigen
IFN	Interferon
IL	Interleukin
ISP	Immature Single Positive
MFI	Median Fluorescence Intensity
MHC	Major Histocompatibility Complex
MRI	Magnetic Resonance Radiation
MS	Multiple Sclerosis

MSSS	Multiple Sclerosis Severity Score
mTEC	Medullary Thymic Epithelial Cells
PBMC	Peripheral Blood Mononuclear Cell
PBS	Phosphate Buffered Saline
PCR	Polymerase Chain Reaction
PECAM	Platelet Endothelial Cell Adhesion Molecule
pMHC	Peptide- Major Histocompatibility Complex
PPMS	Primary Progressive Multiple Sclerosis
qPCR	Quantitative Polymerase Chain Reaction
RRMS	Relapsing-Remitting Multiple Sclerosis
RTE	Recent Thymic Emigrant
S-1-P	Sphigosine-1-Phosphate
sjTREC	Single Joint T-Cell Receptor Excision Circle
SNP	Single Nucleotide polymorphism
SP	Single Positive
TCR	T Cell Receptor
TEC	Thymic Epithelial Cells
TemRA	Effector Memory expressing CD45RA
Th	Helper T-lymphocyte
TREC	T Cell Receptor Excision Circle
VCAM	Vascular Cell Adhesion Molecule
VLA	Very Late Antigen
WHO	World Health Organization

Figure Index

Table Index

1. INTRODUCTION

1.1. Multiple Sclerosis: An Autoimmune Disease from the Central Nervous System

Multiple sclerosis (MS) is one of the most common neurologic diseases worldwide leading to physical and brain disability. It impacts not only the quality of life of the individuals afflicted by the disease but also of their caregivers.

MS is a very heterogeneous autoimmune disease with 3 main forms of progression: the relapsing-remitting (RRMS), the primary progressive (PPMS) and the secondary progressive (SPMS). This stratification is preponderant for the diagnosis and selection of the most adequate therapy to each MS patient.

1.1.1. Worldwide Distribution of Multiple Sclerosis

MS affects twice as many women than men with an average age of disease onset of 30 years-old, an age decisive for family planning and professional career. Dramatically, two decades after diagnosis, nearly 50% of the patients need continued care and use of wheelchair (Dendrou, Fugger, & Friese, 2015; MFIS, 2013).

The most recent reports from World Health Organization (WHO) and from the MS International Federation (MSIF) show that the number of diagnosed individuals has been increasing over the past few years: in 2008, 2.1 million individuals were estimated to be living with the disease worldwide and in 2013 the numbers of estimated cases have increased to 2.3 million. Many factors may be contributing to this increased reported numbers, namely the increased efficiency and acuity on diagnosis, the improvement of available treatments, and concomitantly of patients' survival, and a more accurate reporting and clinical registration of individuals with the disease (MFIS, 2013). Most of the reported cases are in Europe and North America with a considerable percentage of the countries reporting more than 100 patients with MS per 100,000 individuals. In Portugal, it is estimated that approximately 40 per 100,000 individuals are afflicted with MS (Figueiredo, Silva, Cerqueira, Fonseca, & Pereira, 2015).

1.1.2. Historic Overview of Multiple Sclerosis

Although the concept of MS first emerged in 1868 by Jean-Martin Charcot (Kumar, Aslinia, Yale, & Mazza, 2011), it is considered that the first description evocative of MS is the case of Saint Ludwina of Schiedam that dates from the 14th century (Pearce, 2005).

Before being recognized as an individual disease, MS, similarly to other neurologic diseases, was included in the group of the "paraplegias", which comprises all progressive neurologic conditions with motor impairment. Some findings during the 19th century contributed to the individualization of the disease. In 1838, Robert Carswell, a British professor of pathology, described for the first time the disseminated plaques within the nervous system detailing the pathological atrophy of the pons and spinal cord. Concomitantly, the French pathologist Jean Cruveilhier made analogous observations in four autopsies providing a clinical report of one of the cases. In parallel, Charles-Prosper Ollivier published in 1824 on "Traités des maladies de la moelle épinière" the first modern clinical report of MS (Murray, 2009).

The individualization of the disease only became evident when in 1849 the German pathologist Friedrich von Frerichs described what he called of "Hirnsklerose" (brain sclerosis), an illness with motor and visual impairments that he attributed to the occurrence of sclerotic lesions distributed throughout the central nervous system (CNS). The exhaustive pathological and clinic description of the symptomatology and progression of patients with Hirnsklerose combined with the *post-mortem* confirmation of the sclerotic lesions, was the main trigger for the individualization of the disease. However, this idea was not consensually accepted by his colleagues and, in 1868 the clinician Jean-Martin Charcot described what would be the conclusive description of MS (Polman et al., 2011). The contribution of Charcot was enhanced by his detailed histopathological illustrations of the MS lesions and remyelination and demyelination of axons (Kumar et al., 2011).

By the end of the 19th century, the conceptualization of the different phenotypes of MS allowed the stratification of individuals according to their disease form of progression though a consensual and standardized classification was only introduced in 1995 (Lublin, Reingold, & Tiqwa, 1996).

The progressive technological and scientific development allowed a better understanding of MS pathophysiology. Some methodologies such as imaging approaches, namely magnetic resonance imaging, were undoubtedly imperative to understand the disease (Young et al., 1981), as they have allowed the accompaniment of MS activity in the living brain, enabling the disease progression monitoring over time even in the absence of symptoms or in responses to different treatments.

1.1.3. Multiple Sclerosis Etiology

Multiple sclerosis is a chronic disease characterized by the demyelination of neurons that leads to irreversible axonal damage and loss, and progressive neurological disability (Grigoriadis & Pesch, 2015). The immunological process underlying the development of the disease occurs after infiltration of autoimmune T lymphocytes across the brain barriers [the membrane barriers that separate the circulating blood from the brain extracellular fluid in the CNS comprising the blood-brain barrier (BBB) and blood-cerebrospinal fluid barrier] (Minagar & Alexander, 2003). This immunological process has been pointed as the cause of the spatiotemporal occurrence of lesions within the CNS that constitute the hallmark of MS (Dendrou et al., 2015).

Genetic predisposition together with environmental factors associated to individuals' lifestyle have been related with disease penetrance (Beecham et al., 2013; Olsson, Barcellos, & Alfredsson, 2016; Reboul et al., 2000), with epidemiological studies in MS patients families point to genetic and environmental factors (Ebers, Sadovnick, & Risch, 1995). Some studies suggest that genetic variability account for 30% of the risk for developing MS, with over 100 different genetic variants resulting from single-nucleotide polymorphisms (SNPs) (Beecham et al., 2013; Farh et al., 2014; Hemmer, Kerschensteiner, & Korn, 2015; Olsson et al., 2016). Interestingly, the majority of those SNPs are within genes associated with the immune system, including alleles of the human leukocyte antigen (HLA) class II complex, such as the *DRB1*1501* allele (Hoppenbrouwers & Hintzen, 2011); presence of other variants of the HLA class I complex, namely the *A*02* allele, seems to confer protection to MS (Olsson et al., 2016). Concomitantly, SNPs in other genes related to the regulation of the immune response including cytokines, such as interleukin-2 (IL-2), and some interferons (IFNs) or even cytokine receptors including the IL-2Rα and the IL-7Rα, have been reported to be involved in MS (Hartmann et al., 2014; Lundström et al., 2013; Weber et al., 2008).

Although genetic predisposition accounts for around one third of the factors underlying MS development, other factors are required since several monozygotic twins are discordant for MS (Sadovnick et al., 1993). In fact, external factors such as smoking, obesity, viral infections (*e.g.* by the Epstein-Barr Virus), decreased sun exposure and decreased vitamin D levels are described to increase the risk of developing MS. Interestingly, most of these exogenous factors seem to interact with the HLA gene complex and be age dependent, meaning that the risk effect promoted by these factors are more relevant when in a determinate window of the individuals' life, namely, at adolescence (Olsson et al., 2016).

1.1.4. Onset, Progression and Pathophysiology of Multiple Sclerosis

The increased knowledge on MS progression leads to the recurrent organization of committees for re-examination and revision of the diagnostic criteria to improve diagnosis and to better characterize disease progression. Several systems (*e.g.* motor, visual and sensory) provide clinical evidence for MS diagnosis. This coupled with laboratorial data (such as presence of oligoclonal bands on the cerebrospinal fluid, which are present in 90% of the individuals) and/or imaging techniques [such as magnetic resonance imaging (MRI) that allows the detection of abnormalities in the white matter in more than 95% of patients] are preponderant for a correct diagnosis (Compston & Coles, 2008; Filippi et al., 2016).

Currently, three main types of MS can be defined in accordance to the form of progression: relapsing-remitting MS (RRMS), primary progressive MS (PPMS) and secondary progressive MS (SPMS); (**Figure 1.**) (Lublin et al., 2014, 1996). RRMS is the most common form affecting around 85% of the MS patients and is characterized by an acute initial episode of neurologic deficit, also known as clinical isolated syndrome, followed by successive periods of interleaved remission and relapses. These relapses seem to be a consequence of the focal inflammation process occurring at the CNS which is accompanied by myelin degradation, distinguishable by MRI (Compston & Coles, 2008). A period of recovery or remission occur afterwards probably because of neurons' remyelination by oligodendrocytes, leading to clinical improvement. Over time, the capability of recovery observed during the remission phases of RRMS patients decrease, leading to symptoms' aggravation. Therefore, several years after diagnosis (20, in average), individuals develop a progressive form of the disease also called

SPMS (Compston & Coles, 2008). SPMS emerges in approximately 80% of individuals with RRMS and is characterized by CNS atrophy due to axonal loss (Lublin et al., 2014). The inflammatory lesions characteristic of RRMS patients are absent in SPMS individuals.

PPMS appears in 10% of the individuals afflicted by MS. The PPMS onset is around 40 years of age (Tutuncu et al., 2013) and the relapses and remission are not present; instead a progressive accumulation of the disability is observed (Antel, Antel, Caramanos, Arnold, & Kuhlmann, 2012).

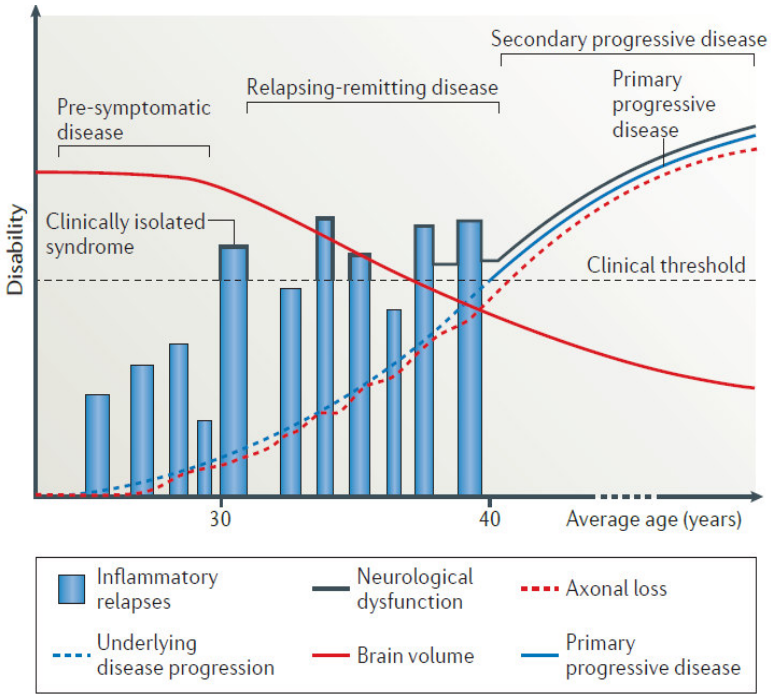

Figure 1. **Progression forms of multiple sclerosis (MS).** Relapsing-remitting (RRMS) is characterized by an initial clinically isolated syndrome followed by interleaved periods of disability and further remission. In most of the cases, RRMS later develop into a progressive form of disease called secondary progressive MS (SPMS) that resembles the primary progressive (PPMS) form. Both SPMS and PPMS are characterized by the progressive accumulation of the disability in the absence of relapse-remitting episodes. Disease progression is accompanied by a decrease in brain volume and axonal loss that lead to cumulative neurologic dysfunction. Adapted from Dendrou *et al.* (Dendrou et al., 2015).

Myelin is a fatty white sheath that surrounds neurons' axons and is produced by oligodendrocytes or Schwann cells in a process called myelination. Myelin is essential for the proper function of the nervous system as it allows saltatory electrical nervous impulse conduction. Events that drive neurons' demyelination ultimately lead to degeneration of axons and neurologic impairment. In MS, demyelination is mediated by immune cells, in particular autoreactive T lymphocytes (Stinissen & Hellings, 2008). Briefly, autoreactive T lymphocytes and other immune cells can enter the CNS and promote local immune response and gliosis (*i.e.* proliferation and activation of glial cells such as microglia, oligodendrocytes and astrocytes) (Minagar & Alexander, 2003). Altogether, these events culminate on myelin destruction and oligodendrocytes' degradation leading to the impaired production of myelin sheaths (**Figure 2.**).

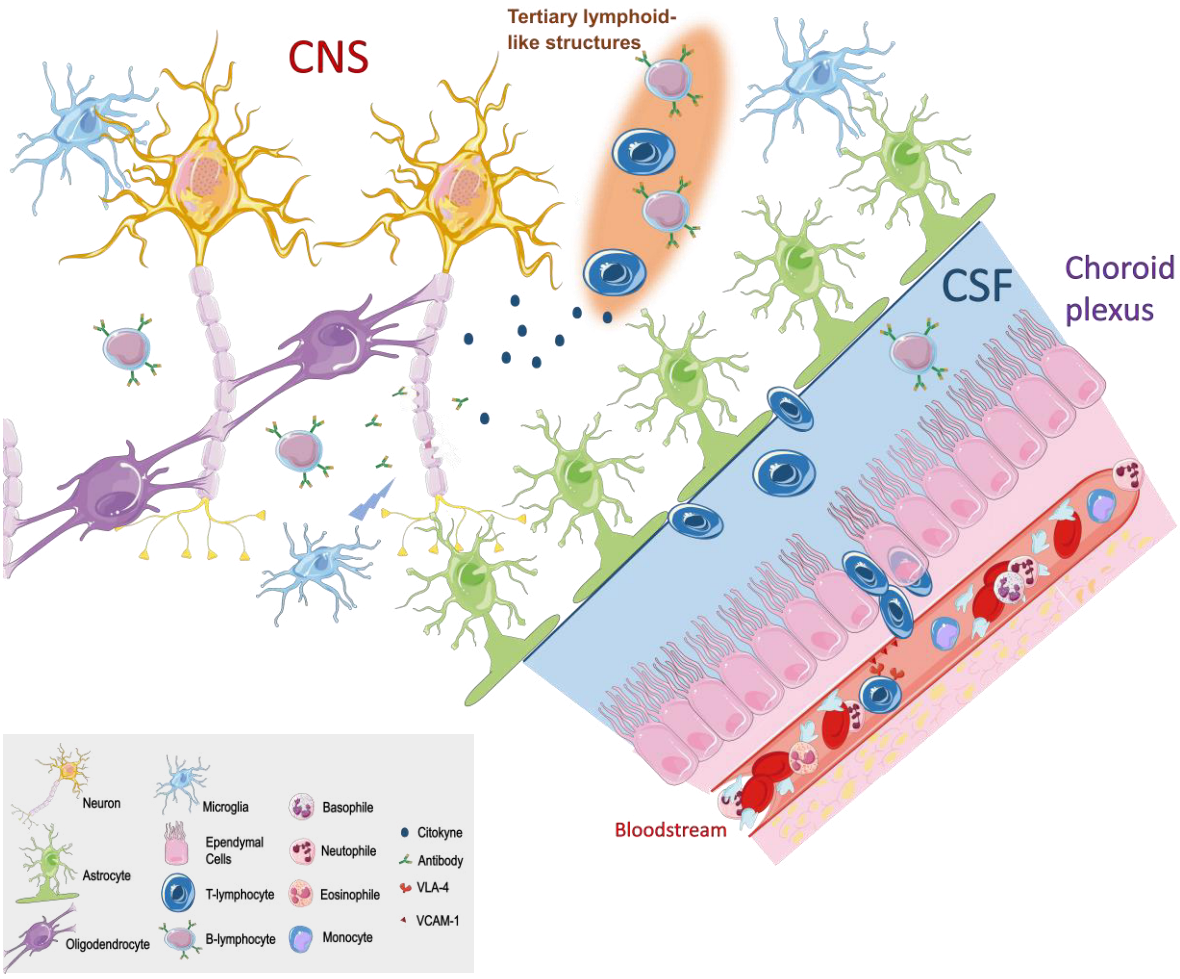

Figure 2. Immunopathology of multiple sclerosis. Immune cells, including T lymphocytes and B lymphocytes, may enter the central nervous system (CNS) through the brain barriers, namely the blood-cerebrospinal fluid brarrier on choroid plexus. Their entrance is facilitated by interaction with specific receptors (e.g. VCAM-1) present in the endothelial cells of the brain barrier. Within the CNS, myelin-reactive T lymphocytes initiate the immune response producing cytokines, which promotes the production of antibodies by B lymphocytes and the activation of microglia and macrophages: this process ultimately leads to the degradation of the myelin sheet. The accumulation of immune cells within the CNS leads to the formation of tertiary lymphoid-like structures. CSF: cerebrospinal fluid.

Although the CNS presents anatomical isolation from the bloodstream, which limits indiscriminate trafficking of cells, increasing evidences show that even in healthy individuals it is possible to find T lymphocytes in the cerebrospinal fluid (CSF) (Engelhardt & Ransohoff, 2005; Engelhardt, Vajkoczy, & Weller, 2017; Shechter, London, & Schwartz, 2013). These cells may play an important role regarding the surveillance of the CNS as they will interact with the existing antigen-loaded innate immune cells within the CNS. These innate cells may present antigens to the autoreactive T lymphocytes leading to the initiation of an inflammatory process within the CNS (McMahon, Bailey, Castenada, Waldner, & Miller, 2005).

Currently, one of the main challenges in what concerns MS development resides on the lack of knowledge regarding the site of disease onset: in the periphery or within the CNS. The model describing the onset of MS within the CNS postulates that other cells, apart from the autoreactive T lymphocytes, may trigger the disease and that infiltration of the autoreactive cells may be a later and secondary phenomenon. Inflammatory responses against intra-CNS infectious agents or processes underlying neurodegeneration have been suggested as the mechanisms that could trigger MS initiation within the CNS (Olson & Miller, 2004). The other model resides on the hypothesis that peripheral autoreactive T lymphocytes may be the initiators of MS (Fletcher, Lalor, Sweeney, Tubridy, & Mills, 2010); after escaping the existing tolerance mechanisms in the thymus and/or in the periphery, the autoreactive T lymphocytes can be activated by several different mechanisms (i.e. bystander activation, molecular mimicry) and then remain in the bloodstream and/or enter the CNS and induce tissue damage. This ultimate model is supported by the experimental autoimmune encephalomyelitis (EAE) model in mice for which myelin antigens emulsified in adjuvants are administered to activate autoreactive T lymphocytes (Fletcher et al., 2010). These cells may then exert their effector functions on the CNS after infiltration through the brain barriers.

Upon these facts, it seems reasonable that the increased knowledge on the T lymphocytes development and the selection of cells in the thymus may highlight the mechanisms behind the initiation and progression of MS.

1.2. T Lymphocytes: From Thymic Differentiation to Peripheral Subsets

The thymus is the organ responsible for the differentiation of T lymphocytes. Several mechanisms occurring in the thymus during T lymphocytes' differentiation are essential to generate self-restricted and self-tolerant T lymphocytes (central tolerance).

As T lymphocytes are exported from the thymus, they play key roles regarding the adaptive immune response. As a very heterogeneous population, T lymphocytes can be divided into several cell subsets in accordance to their phenotype and function which depends on their experience in the periphery, maintaining their naïve or changing to effector or memory phenotypes.

1.2.1. Thymic T Lymphocytes' Differentiation

The thymus is the organ where hematopoietic T lymphocytes' precursors differentiate into T lymphocytes (Gameiro, Nagib, and Verinaud 2010). Located immediately above the heart, the thymus can be fractionated into four main regions: the medulla, the cortico-medullary junction, the cortex and the subcapsular zone. These regions sustain different specialized cells that provide specific microenvironments that support proliferation, maturation and selection of thymocytes (Boehmer & Melchers, 2010).

Bone marrow precursors enter the thymus through the post-capillary venules at the cortico-medullary junction, located between the medullary and cortical regions (Prockop & Petrie, 2004). This process is dependent on the availability of unoccupied intrathymic niches, in a process mediated by the expression of P-selectin by the thymic endothelium that binds to PSGL-1 expressed by thymocyte precursors (Rossi et al., 2005). Upon entering the thymus, thymocytes migrate outward within the cortex and back to the medulla passing through the cortico-medullary junction in a process driven by differences in chemokines' pattern (Benz, Heinzel, & Bleul, 2004).

As cells migrate through the thymus, they go through different stages of differentiation that can be characterized by different markers, being the most commonly used the CD3, CD4, CD8, CD44 and CD25 (Benz et al., 2004; Misslitz et al., 2004). The most immature thymocytes are the double negative cells (DN), as they lack the expression of CD4 and CD8, as well as of CD3. In mice, four different subsets of DN cells can be distinguished in accordance to the expression of CD25 (the IL-2 receptor) and CD44 (cell surface glycoprotein important for cell interactions, adhesion and migration). The most immature DN subset (DN1) is $CD44^{+}CD25^{-}$; as thymocytes migrate throughout the cortex, they gain the CD25 marker ($CD44^{+}CD25^{+}$; DN2), followed by a subset characterized by the absence of CD44 ($CD44^{-}CD25^{+}$; DN3). DN3 are localized at the outermost region of the cortex, the subcapsular zone. The most mature double negative population (DN4) is characterized by the absence of both markers ($CD44^{-}CD25^{-}$) (Germain, 2002). After the DN stage, a transitory cell subset characterized by the expression of the CD4 marker can be found, also called CD4 immature single-positive (CD4 ISP), which are immediate precursors of the double positive thymocytes (DP; $CD4^{+}CD8^{+}$; **Figure 3.**). Notwithstanding in humans the four DN subsets are not evident (Gameiro et al., 2010), it is at the late

DN and CD4 ISP stages that the V(D)J rearrangement of the T cell receptor (TCR) γ, δ and β loci take place giving rise to two distinct T lymphocyte lineages expressing either the αβTCR or γδTCR (Dik et al., 2005). As the αβT lymphocytes are the cells addressed in this thesis, from now on we will focus on this cell subset and refer to them simply as T lymphocytes. Upon rearrangement of the TCR and its expression on the cell surface, DP thymocytes are selected accordingly to the ability of their TCR to interact with peptide-major histocompatibility complex (MHC) complexes (pMHC) expressed by cortical thymic epithelial cells, dendritic cells and macrophages, among other antigen presenting cells. Thymocytes whose TCRs are not able to interact with the pMHC do not receive survival signals and dye by neglect; only thymocytes that bind to the pMHC with sufficient avidity proceed to further differentiation and maturation in a processed termed positive selection (Klein, Hinterberger, Wirnsberger, & Kyewski, 2009; Klein, Kyewski, Allen, & Hogquist, 2014). Thymocytes positively selected are chemoattracted to the medulla and continue differentiation to become either CD4 single-positive (CD4SP) or CD8 single-positive (CD8SP) (Kwan & Killeen, 2004; Takahama, 2006). At this stage, thymocytes that recognize and bind pMHCs with too high avidity die by apoptosis (Klein et al., 2009) in a process called negative selection. Negative selection is crucial to limit the full differentiation of autoimmune T lymphocytes (Klein et al., 2014). In the end, a repertoire of T lymphocytes whose TCR are mostly self-restricted (able to recognize self-MHC) and self-tolerant (able to tolerate self-pMHC) is generated and exported to the periphery at the cortico-medullary junction.

This process of generating self-tolerant T lymphocytes within the thymus is referred to as central tolerance. This process is complemented by a peripheral mechanism called peripheral tolerance, mostly mediated by regulatory T cells (Richards, Kyewski, & Feuerer, 2016). The two mechanisms are essential to control potentially autoreactive T lymphocytes that egress from the thymus.

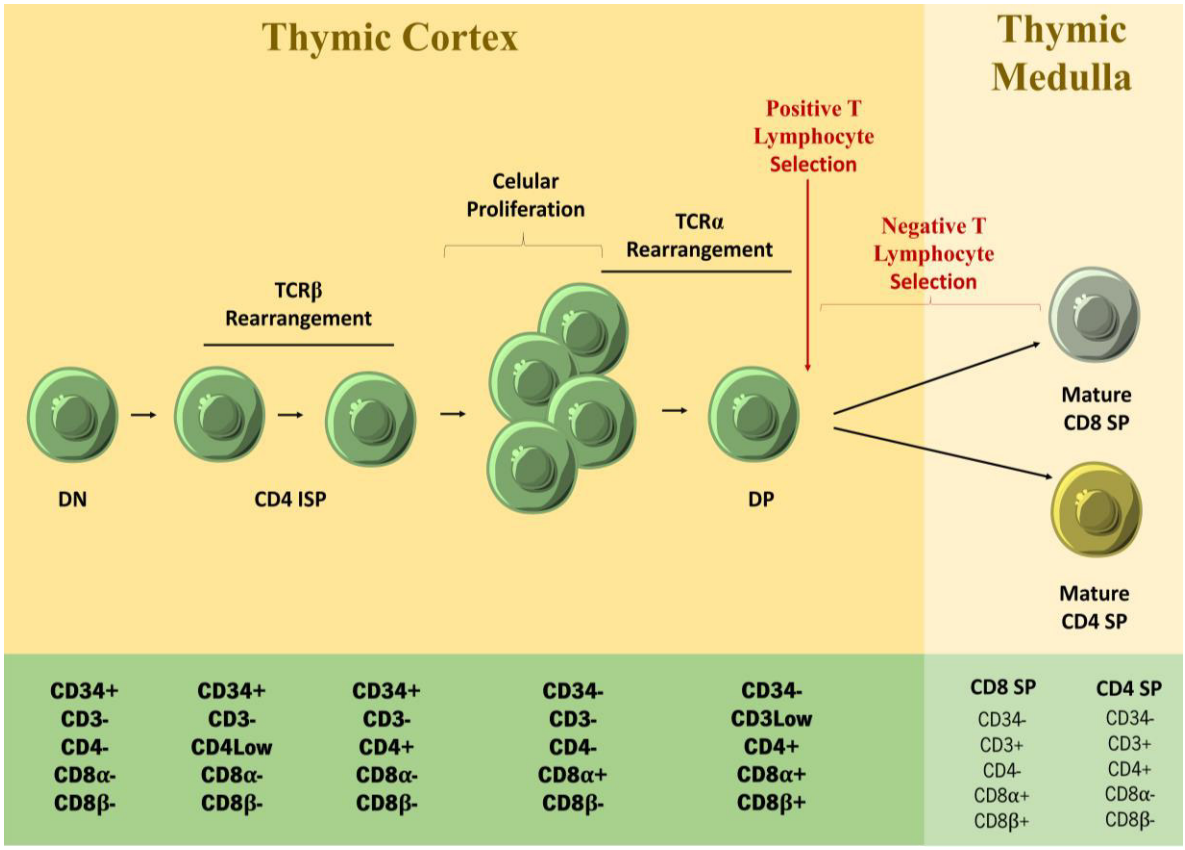

Figure 3. Maturation of precursor T lymphocytes within the thymus. Bone marrow precursors enter the thymus as double negative cells (DN; $CD4^-CD8^-$) at the cortical-medullary region. The expression of CD4 initiates and cells are considered immature single positive (CD4 ISP). Concomitantly, occurs the rearrangement of the β-loci of the TCR and further selection of the cells that succeed the rearrangement. A period of great cellular proliferation occurs before the rearrangement of the α-loci of the TCR. Concomitantly, cells initiate the expression of the CD8 surface marker and, therefore, cells are called double positive (DP; $CD4^+CD8^+$). Only cells containing a functional TCR capable of recognizing and bind, non-covalently, to the pMHC proceed development (positive T lymphocyte selection). As cells migrate from the cortex to the medulla, maturation of lymphocytes occurs and they become single positive (SP; $CD4^+$ or $CD8^+$). As cells migrate, the contact with thymic endothelial cells dictates survival of lymphocytes – lymphocytes with high affinity to the MHC do not receive signals for survival and are eliminated by apoptosis. During maturation, precursor T lymphocytes present different phenotypes characterized by expression of different surface markers (green board).

1.2.2. Thymic Function Evaluation in Humans

Currently no direct method to estimate thymic function is available for humans and, therefore, several surrogates are used to determine thymic contribution to peripheral T lymphocytes. Since each of the existing surrogates for thymic function present limitations, different surrogates should be combined to have a more accurate estimation of thymic function. Thymic function surrogates include quantification of recent thymic emigrants (RTEs) in the blood, quantification of sj/β T cell receptor excision circles (sj/βTRECs) in the blood, evaluation of thymic volume and index (an indicator of active thymic tissue) by Chest Computed Tomography (CT) scan or by evaluation of the metabolic activity of

the thymus (upon radiolabeled glucose uptake) Positron Emission Tomography (PET), among others. These techniques are mostly used for research proposes.

During TCR rearrangement, the excision of portions of DNA takes place to give rise to a functional and unique TCR. After excision, the DNA is circularized in stable episomal T lymphocytes excision circles (TRECs) (Serana et al., 2013). The excision of the δ, located within the α loci, gives rise to the single-joint TRECs (sjTRECs) which are present in approximately 70% of the cells exported from the thymus, while the rearrangement on the β locus gives rise to the βTREC, which occurs during the later DN/CD4ISP stage (M. Dion, Sékaly, & Cheynier, 2007). As episomal DNA, TRECs do not replicate and, therefore, both β and sjTRECs containing T-lymphocytes are progressively diluted-out during T lymphocyte peripheral proliferation (M. Dion et al., 2007). After the generation of a productive β-chain pre-TCR and before the generation of sjTREC, a period of increased proliferation and development occurs. Therefore, estimation of the sj/βTRECs is an indicator of intrathymic proliferation and, because this ratio it is not affected by peripheral proliferation, contrarily to each TREC alone, the sj/βTRECs can be used as a surrogate for thymic function

Despite specific markers that allow the discrimination between RTEs from the rest of the peripheral T lymphocytes pool are available, it is known that RTEs present high expression of the transmembrane glycoprotein CD31 (also known as PECAM-1) (Fink, 2012; Hazenberg, Verschuren, Hamann, Miedema, & Dongen, 2001; Junge et al., 2007) and that its expression wanes as these cells divide in the periphery (Demeure, Byun, Yang, Vezzio, & Delespesse, 1996). In fact, it was shown that the higher the CD31 expression on naïve T lymphocytes, the higher the proportion of TREC containing cells (Junge et al., 2007). Furthermore, protein tyrosine-kinase 7 (PTK7) has also been pointed as a possible surface marker for RTEs, however its use is controversial as a study suggests that this marker does not necessarily reflect RTEs numbers (Bains, Yates, & Callard, 2013).

1.2.3. Peripheral T Lymphocytes' Subsets

After maturation within the thymus, cells are exported to the periphery as naïve T lymphocytes. In humans, these cells are phenotypically characterized by the expression of CD45RA and the lymph node homing receptors CCR7 and CD62L (**Figure 4.**) (Förster et al., 1999).

Naïve T lymphocytes are unable to produce effective responses to protect against infections. For that reason, they need to be primed via the interaction of their TCR with the cognate-pMHC expressed on the cell surface of antigen presenting cells (Sprent & Surh, 2011). This process leads to the activation of the naïve T lymphocytes and consequent down-regulation of CD45RA expression and up-regulation of the CD45RO isoform (Johannisson & Festin, 1995; Pinto, Covas, & Victorino, 1991). Upon activation, an heterogeneous population of memory T lymphocytes can be identified and different subsets defined based on the characteristic phenotype, tissue-homing capacity and function: central memory (CM), effector memory (EM) and the terminally differentiated T lymphocytes (also called EM with re-expression of the CD45RA marker, or T_{EMRA}) (Sallusto, Lenig, Förster, Lipp, & Lanzavecchia, 1999). Phenotypically, both CM and EM T lymphocytes express the CD45RO isoform, but not CD45RA, and the former has lost the lymph node homing receptor CCR7 (Sallusto et al., 1999). As EM lack CCR7 expression, they preferentially home to mucosal sites and tissues. Additionally, in comparison to CM, EM T lymphocytes seem to be more differentiated and present lower self-renewal capacity, decreased proliferative profile and are more potent producers of effector cytokines (Mahnke, Brodie, Sallusto, Roederer, & Lugli, 2013; Maus et al., 2004). As for the T_{EMRA} subset, these are more abundant within $CD8^+$ T lymphocytes and, although they express the CD45RA but not the CD45RO isoform, they seem to be the most differentiated subset among the memory T lymphocytes. T_{EMRA} present decreased proliferative capability and low functional activity (**Figure 4**).

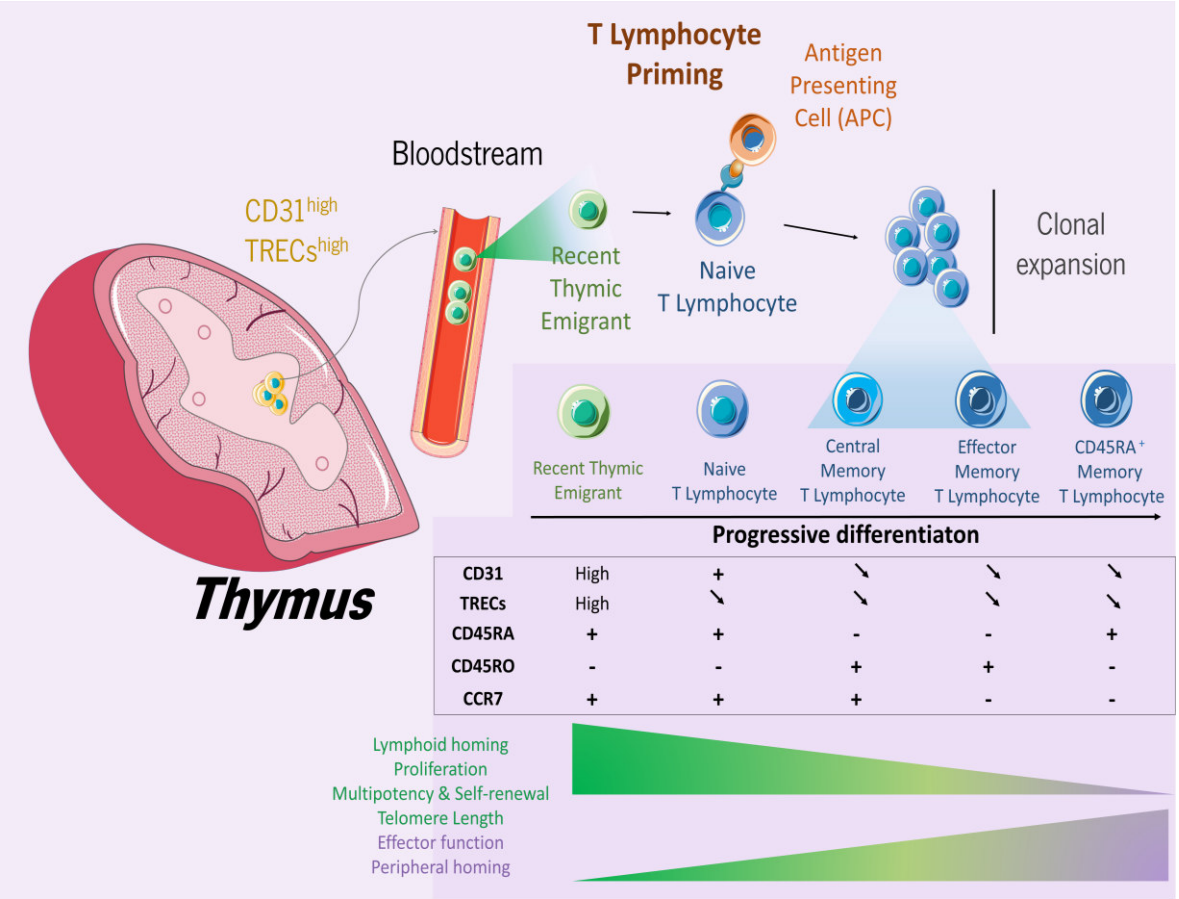

Figure 4. T lymphocytes priming and progressive differentiation. Recent thymic emigrants (RTE) are exported from the thymus to the periphery presenting high expression of CD31 and content of TRECs. Before activation through encounter with the cognate antigen presents by antigen present cells, T lymphocytes are considered naïve. Upon activation, T lymphocytes are activated, are clonally expanded and differentiate into memory. Two main subsets of memory can be distinguished: central memory (CM) and effector memory (EM) T lymphocytes. Some EM T lymphocytes can re-express CD45RA isoform and are termed terminally differentiated or TemRA. The different subsets of naïve and memory present different expression of surface markers, length of telomere repeats and proliferative capacity as well as, different multipotency, self-renew, homing and effector capacity.

1.2.4. Thymic Involution and Immune System's Aging

Thymic involution starts early in life and occurs as a natural process associated to the replacement of the thymic epithelial space (*i.e.* cortex and medulla) by adipose tissue. This thymic involution, associated with the reduced seeding of the thymus with bone marrow precursors and the decrease in thymic niches leads to reduction or even abrogation of T lymphocyte differentiation with age (Linton & Dorshkind, 2004).

Age-related changes on the peripheral immune system occur mainly due to a diminished exportation of RTEs by the involuted thymus. As a consequence, the numbers of naïve T lymphocytes

in the periphery are decreased and an enrichment of the memory compartment over the naïve is observed (Geiger & Rudolph, 2009; Naylor et al., 2005). This might potentially lead to a reduced capability of T lymphocytes to develop immunological memory to new antigens (Farber, Yudanin, & Restifo, 2013; Saule et al., 2006). Besides that, as thymus involutes and immune system ages, the proportions of $CD8^+$ and $CD4^+$ T lymphocytes subsets is altered (Briceño et al., 2016; Naylor et al., 2005).

With age, the immune system tends to accumulate aged T lymphocytes that, as several other cell types, present reduced telomere length (Akbar & Vukmanovic-Stejic, 2007; Allsopp et al., 1995). Telomeres constitute the cap portion on the extremity of the chromosomes, conferring protection to the internal coding portion. As cells proliferate in normal conditions, telomeres undergo natural abrasion. Since cells in a later stage of differentiation comprise shorter telomeres, naïve T lymphocytes present the longer telomeres, followed by CM, EM T lymphocytes and finally T_{EMRA}. Interestingly, in autoimmune diseases an accumulation of end-stage senescent cells has been observed (Georgin-Lavialle et al., 2010).

1.3. Immunosenescence in Multiple Sclerosis and Immunomodulatory Drugs

As the immune system ages, immune cells capability to recognize new foreign antigens tends to be reduced and maintenance of tolerance mechanisms to self-antigens tends also to become reduced, increasing the probability to develop autoimmune diseases (Gonsette, 2012; Hug et al., 2003). Interestingly, previous data obtained from phenotypical evaluation of $CD4^+$ T lymphocytes subsets (RTEs, naïve and memory) through flow-cytometry suggested that children with RRMS present decreased RTEs and naïve to memory ratio and, therefore, increased immune system aging when compared to age-matched healthy individuals (Balint et al., 2013; Correia, Augusto, Meireles, Pinto, & Sousa, 2016; Vargas-Lowy & Chitnis, 2012). In adults, it has been described that, in comparison to healthy controls, RRMS patients also present decreased number of TRECs, determined by nested-PCR, and RTEs, quantified by flow-cytometry, which suggests impaired thymic function and consequently impaired T lymphocytes homeostasis and immune tolerance (Duszczyszyn et al., 2010; Hug et al., 2003). In what concerns PPMS patients, those were also reported to have reduced number of TRECs as well as of RTEs indicting decreased thymic output and alterations in T lymphocytes subsets in

comparison to RRMS and healthy controls (Haegert et al., 2011). Interestingly, some findings point to an increase of peripheral homeostatic T lymphocytes' proliferation as a mechanism to compensate for the premature thymic atrophy (M. L. Dion et al., 2004; Duszczyszyn et al., 2006), which may predispose MS individuals to increased autoreactivity of T lymphocytes (Duszczyszyn et al., 2010).

As immune cells present an essential role in MS pathophysiology, several immunomodulators have been developed to treat this disease such as Natalizumab, Teriflunomide or Fingolimod. These drugs act mainly on immune system cells to reduce their activation, proliferation or even access to the CNS.

The existing immunotherapeutic agents, however, fail to treat the progressive forms of MS and are mostly used to treat RRMS patients (Feinstein, Freeman, and Lo 2015). Currently several immunomodulatory drugs to treat the progressive forms are being clinically tested, namely the monoclonal antibody ocrelizumab that targets $CD20^+$ B lymphocytes and leads to their destruction (Montalban et al. 2016).

Altogether this raises the need for a better knowledge about the development of the different forms of the disease. Therefore, it is very important to study and make efforts to unravel how this thymic function and immune system aging correlate with the development of the different MS progression forms. Currently, several strategies for boosting thymic function and, consequently improve immune system reconstitution, are under clinical trials ((Chaudhry, Dudakov, Brink, & Brink, 2016; Nunes-Cabaço & Sousa, 2013)). If proven that individuals with different MS progression forms present distinct thymic funtion, therapies based on the modulation of its function could be adapted and adopted to treat those patients.

2. OBJECTIVES

The central hypothesis of this research work is that thymic function and immune system aging, namely of T lymphocytes, have an essential role on the pathophysiological process that characterizes MS. Since the mechanisms that trigger the development of this autoimmune disease, and what dictates the distinct forms of progression, are still to be elucidated, it becomes pertinent to study the thymus and the immune aging of these cells on the periphery.

The goal of this project is to investigate how thymic function in MS individuals correlates with peripheral T lymphocyte aging and with different MS progressing forms. More specifically, the strategy was:

1. Estimate thymic function through the quantification of RTE and TRECs;
2. Evaluate the immune system aging through determination of the naïve to memory ratio on T lymphocytes and by the quantification of T lymphocytes relative length of telomere repeats.

3. MATERIAL AND METHODS

3.1. Study population

Patients living in the Minho Region of Portugal, followed-up as outpatients at *Hospital de Braga*, diagnosed with MS in accordance to the McDonald criteria, with a past reliable medical record of MS disease-course and older than 18 years old were provided an explanation of the study and invited to take part on the cohort. Those who agreed to participate have signed an informed consent (project approved by the *Comissão de Ética para a Saúde do Hospital de Braga*). RRMS participants were either treatment-naïve or at stable treatment with a single disease-modifying drug for at least 6 months, and PPMS patients were treatment-naïve. Individuals with other immune disorders (autoimmune diseases or immunodeficiency syndromes), under corticosteroids (in the last 3 months or continuously for more than 6 months in the past) or other immunosuppressive drugs (*e.g.* cladribine, methotrexate, azathioprine, mycophenolate, cyclophosphamide, mitoxantrone, etc.), history of radiotherapy and/or chemotherapy for cancer, submitted to splenectomy or thymectomy, pregnant were excluded from the study. Data on age, gender, type of the disease and severity [estimated by the last MS severity score (MSSS)], date of diagnosis, total number of relapses since the onset of the disease, last expanded disability status scale (EDSS) value, date of the last EDSS, current treatment, date of the last corticoid treatment (if applicable) and regular medication were retrieved from patients' medical file (**Table 1.**). Age and gender match healthy controls were selected from on-going studies and included in this study (Horta et al., 2013; Nobrega et al., 2016).

Table 1. Demographic and clinical characterization of the cohort.

	RRMS		PPMS	Controls
	Treatment-naïve (n=4)	On treatment (n=32)	(n=18)	(n=28)
Median age, years (range)	33 (24-45)	40 (22-61)	36 (36-76)	41 (22-64)
% Men (n)	0 (0)	34.4 (11)	44.4 (8)	25 (7)
Median age of MS onset, years (range)	33 (24-45)	30.78 (14-54)	52.63 (35-69)	na
Median duration of MS, years (range)	0[a)]	8.94 (0-21)	6.63 (0-19)	na
Mean last EDSS (range)	0.3 (0-1)	2.7 (0-6.5)	4.9 (3.5-7.5)	na
Disease modifying drugs (n)	na	Natalizumab (n=23); Fingolimod (n=4); Teriflunomide (n=4); IFN-β (n=1)	na	na

[a)] These patients entered the study in the moment they were diagnosed with MS. na, not applicable; EDSS, Expanded Disability Status Scale.

3.2. Sample Processing

Blood was collected into EDTA tubes and processed on the same day. Peripheral blood mononuclear cells (PBMCs) were isolated from blood using the Histopaque-1077 gradient solution (Sigma-Aldrich, St. Louis, MO, USA) upon centrifugation at 400g for 30 minutes, at room temperature, in accordance to manufacturer's instructions. After two washes using phosphate buffered saline (PBS), cells were resuspended in RPMI media supplemented with 10% heat-inactivated fetal bovine serum (FBS; both Merck Millipore, Darmstadt, Germany) and counted using trypan blue exclusion dye. Two vials, containing 1 million PBMCs each, were centrifuged at 12470g; supernatant was removed and a dry pellet was frozen at -80°C for TRECs quantification. The remaining cells were adjusted to a final concentration of 5 million cells/mL in RPMI media supplemented with 20% FBS and 10% dimethyl sulfoxide (DMSO; Sigma-Aldrich); one vial containing 2.5 million PBMCs was cryopreserved (used for multiparametric analysis by flow cytometry) and the remaining PBMCs were aliquot in vials containing 5 million PBMCs each (used for flow-FISH or cell banking).

3.3. Characterization of the T Lymphocytes' Subsets

A single vial per individual containing 2.5 million PBMCs was rapidly thawed and washed twice using FACS buffer [PBS supplemented with 0.3% bovine serum albumin (BSA), 0.01% NaN_3 and 2mM Na_2EDTA). One million cells was used for T lymphocytes subsets evaluation using the following combination of monoclonal antibodies: PE-conjugated anti-human CD3 (clone OKT3); APC-Cy7-conjugated anti-human CD4 (clone RPA-T4); APC-conjugated anti-human CD8 (clone RPA-T8); BV510-conjugated anti-human CD45 (clone HI30); Pacific Blue-conjugated anti-human CD45RA (clone HI100); BV650-conjugated anti-human CD45RO (clone UCHL1); PeCy7-conjugated anti-human CD31 (clone WM59); FITC-conjugated anti-human CD19 (clone HIB19) and BV785-conjugated anti-human CCR7(clone G043H7; all purchased from BioLegend, San Diego, CA, USA). The optimal concentration of each antibody was determined by testing serial dilutions. After incubation of PBMCs with the antibodies mix (15 minutes in the dark at room temperature), cells were washed once with FACS buffer. The 7AAD dead cell exclusion dye (BioLegend) was added 10 minutes before acquisition of the samples on a BD LSRII flow cytometer (equipped with a blue 488nm, a red 633nm and a violet 405nm lasers) using the FACS Diva Software (Becton Dickinson, Franklin Lakes, NJ, USA). Data were analyzed as described in the results section (section **4.1.3.**), using the FlowJo Software version 10 (Tree Star,

Ashland, OR, USA). Rainbow calibration particles (BioLegend) were used in all acquisitions to maintain the standardization of the cytometer settings between experiments.

3.4. Flow-Cytometry Fluorescence *in Situ* Hybridization (Flow-FISH)

The relative length of telomere repeats can be determined by fluorescence *in situ* hybridization (FISH) using labeled peptide nucleic acid (PNA) probes specific for telomere repeats (TTAGGG). Measurement of the fluorescent signal (that is proportional to the number of repeats) is achieved by flow-cytometry (flow-FISH). This technique was implemented in the laboratory in the context of this MSc project, based on a protocol described by others (Baerlocher, Vulto, de Jong, & Lansdorp, 2006). Bovine thymocytes were added to each sample (on average they have 2 to 3-times longer telomere repeats than human cells) and were used as an internal reference; the inclusion of a human internal control and the use of calibration beads at each acquisition allows the determination of the constancy of the analysis between experiments.

3.4.1. Bovine Thymocytes Isolation

Fresh bovine thymus was obtained from a slaughterhouse where it was immediately placed on a container with RPMI media supplemented with 5% FBS, 1% Heparin (Sigma-Aldrich) and 0.02mg/mL DNase (Roche Applied Science, Mannheim, Germany) for transportation. After removing most of the visible fat tissue, the thymus was finely minced with scalpels and forced to pass through a strainer. The obtained cell suspension was washed twice with PBS containing 0.02mg/mL DNase (centrifugations at 450g, 10 minutes, 4°C) and resuspended in PBS. Cell clumps were left to sediment and, 2 minutes after, supernatant was recovered and mixed with 0.2% of formaldehyde in PBS in a 1:1 proportion. Cells were incubated for 10 minutes, in a shaker, and afterwards spin-down for 5 minutes at 450g. Cell pellet was resuspended in PBS to a final concentration of 50 million cells/mL; ice-cold freezing solution (80% FBS and 20% DMSO) was added to the cell suspension in a 1:1 proportion, aliquot 1mL per cryovial and stored at -80°C.

3.4.2. Estimation of the Relative Length of Telomere Repeats on T Lymphocytes

Frozen fixed bovine thymocytes and a single vial per participant containing 5 million PBMCs were rapidly thawed at 37°C and washed once with PBS. Vials containing a mixture of 0.4 million bovine thymocytes and 1 million PBMCs were prepared in quadruplicate per individual. Samples were washed once with FACS buffer and incubated with biotinilated anti-human CD3 (clone OKT3) and purified anti-human CD4 (clone A161A1, both purchased from BioLegend). After 20 minutes in the dark at room temperature, samples were washed with FACS buffer. Samples were resuspended in 0.1mL of 4mM BS^3 [bis(sulfosuccinimidyl) suberate; Thermo Fisher Scientific, MA, USA] and incubated at 4°C for 30 minutes in the dark; 8µL of 1M Tris buffer pH 7.8 was added and further incubated for 15 minutes at room temperature. Cells were washed once with ice-cold PBS and afterwards with hybridization buffer (0.1% BSA, 10mM HEPES, 0.05g/mL D-glucose) before being incubated with Alexa-Fluor 488-conjugated PNA Telomere-C probe (CCCTAA, PNAbio, Newbury Park, CA, USA) at room temperature for 10 minutes in the dark, followed by another incubation period at 85°C for 15 minutes in the dark. Samples were left to hybridize at room temperature for 120 minutes in the dark; from each quadruplicate tubes per patient, 3 were incubated with the probe and the forth without probe (hybridization buffer only). Samples were washed twice with washing solution A (14mM Tris, 0,1% BSA, 0,1% Tween20 and 75% formamide) followed by a washing step using washing solution B (10mM HEPES solution, 0.1% Tween20, 0.1% BSA and 4.4% D-glucose) and another with FACS buffer. Samples were incubated at room temperature for 20 minutes in the dark, with BV421-conjugated streptavidin, PE-conjugated goat anti-rat IgG and BV510-conjugated anti-human CD45 (clone HI30; all from BioLegend); the optimal concentration of each antibody was determined by testing serial dilutions. Finally, cells were washed once with FACS buffer and acquired on the flow cytometer (as described above on section **3.3.**) and the analysis performed as described in the results section (section **4.1.2.**)

3.5. Quantification of T Cell Receptor Excision Circles (TRECs) by Nested-PCR

The proportion of T lymphocytes on the peripheral blood that present TRECs is scarce and for this reason, sensitive techniques are required for TREC quantification. Dion *et al.* has described a Nested-PCR protocol suitable for the quantification of these molecules (M. Dion et al., 2007), and efforts to implement this protocol in the laboratory were made in the context of this MSc project. Briefly, using a

specific set of primers for the target sjTREC sequence and for the housekeeping CD3 gene on a single reaction mix, a conventional polymerase chain reaction (PCR) was performed to achieve a first amplification step. An aliquot of the conventional PCR amplicon was used as a template for a second round of amplification by quantitative PCR (qPCR) for each of the genes in separate reaction tubes. A known concentration of a plasmid containing a single copy of each of the genes (CD3γ and TREC) was used as reference to determine the concentration of TRECs per individual.

3.5.1. Cell Lysis and DNA Extraction

The dry pellets containing 1 million PBMCs were thawed at room temperature for 10 minutes and resuspended in 0.1mL lysis buffer [10mM Tris-HCl pH 8.0, 0.05% Tween 20, 0.05% NP40 and 200µg/mL of proteinase K (Grisp)]. Samples were incubated in the thermocycler [Mastercycler epgradient S (Eppendorf, Hamburg, Germany)] with the following program: 56°C for 30 minutes; 98°C for 10 minutes; 20°C forever. Afterwards, samples were stored at 4°C until being used.

3.5.2. Quantification of T Cell Receptor Excision Circles

Precisely 10uL of cell lysate from each patient, plasmid or water (negative control) were amplified by conventional PCR in a final volume of 100µL as follows: 1µM sjTRECs OUT 3' primer (5'-ACATTTGCTCCGTGGTCTGT-3'); 1µM sjTRECs OUT 5' primer (5'-CTCTCCTATCTCTGCTCTGAA-3'); 1µM CD3γ OUT 3' primer (5'-AGCTCTGAAGTAGGGAACATAT-3'); 1µM CD3γ OUT 5' primer (5'-ACTGACATGGAACAGGGGAA-3'; all from Thermo Fisher Scientific); 3.5mM $MgCl_2$; 0.2mM dNTP mix; Taq buffer 1X; 0.044U/µL Xpert Taq DNA Polymerase (all from Grisp), all diluted in PCR-grade water. Tubes were placed in the thermocycler and the following program was used: 95°C for 15 minutes (initial complete denaturation of DNA template), followed by 18 amplification cycles of 95°C for 30 seconds (denaturation), 60°C for 30 seconds (annealing) and 72°C for 3 minutes (extension). Samples were stored at 4°C until being used.

Samples' amplification products from the conventional PCR were 10-fold diluted in PCR-grade water; a standard curve with 8 sequential 10-fold dilutions of the plasmid's amplification product was prepared. Two distinct qPCR reaction mixtures were prepared per sample/plasmid/negative control: one mixture containing primers directed for CD3γ amplification and another with primers directed for sjTREC. Each of the mixtures contained the following components: 1X Kapa SYBR FAST qPCR Kit

Master Mix Universal (Kapa Biosystems, Wilmington, Massachusetts, USA), 1.43µM sjTRECs IN 3' (5'-GTGCTGGCATCAGAGTGTGT-3') and 1.43µM sjTRECs IN 5' (5'-TGATGCCACATCCCTTTCAA-3') primers or 1.43µM CD3γ IN 3' (5'-CCTCTCTTCAGCCATTTAAGTA-3') and 1.43µM CD3γ IN 5' (5'-GGCTATCATTCTTCTTCAAGGTA-3'; all from Thermo Fisher Scientific) primers, all diluted in PCR-grade water. Exactly 4µL of the diluted products of the conventional PCR were added to each well for each gene and the calibration curve was performed in duplicate for each gene. Samples were run on a Bio-Rad CFX96 real-time system with a C1000 thermal cycler (Bio-Rad, Hercules, California, USA) using the following program: 95°C for 15 minutes (initial denaturation and Taq polymerase activation) followed by 40 cycles of 95°C for 2 seconds (denaturation), 55°C for 15 seconds (annealing) and 72°C for 10 seconds (extension). The fluorescence signal was measured in each well at the end of each cycle and all melting curves exhibited a single sharp peak at a temperature characteristic of the primers used. Data were analyzed in Bio-Rad CFX Manager version 3.1 (Bio-Rad).

After obtaining a standard curve with a slope between 3.2 and 3.4 (minimal margin of error defined – $2^{3.325}=10$, which corresponds to the theoretical dilution factor between points), the concentration of TRECs and CD3γ was determined in accordance to the cycle of its amplification (Cq) and using the standard curve obtained. The concentration of TRECs corresponds to the division of the TRECs frequency by the CD3γ frequency. The value obtained was then multiplied by 2, corresponding to the two allelic copies of each TREC existing in each cell, and by 10^5 (the initial number of cells used for the analysis).

3.6. Statistical Analysis

The question hypothesized in this study is that thymic function and immune system aging could be impaired in the different forms of progression of multiple sclerosis in comparison to healthy control individuals. To test for statistical differences in gender and age between the MS groups and the healthy controls and, a Fisher's exact qui-squared test and a one-way analysis of variance (ANOVA), or its equivalent non-parametric Kruskal-Wallis test, respectively, to determine the gender and age, respectively, of the healthy individuals to include in the study. Furthermore, the effect of different treatments on the percentage of several T lymphocytes subsets was also compared through an ANOVA or Kruskal-Wallis followed by Bonferroni's or Dunn's multiple comparison tests, respectively.

To evaluate whether the distribution was normal or not a Shapiro-Wilk test of normality was performed since it is an adequated test for small size samples.

To correlate the percentages of the T lymphocytes' subsets with age in MS patients and healthy individuals a Pearson's correlation coefficient test or its equivalent non-parametric Spearman's rank coefficient test was performed on sample with normal or non-normal distribution, respectively. To evaluate the predictors for the percentages of the different T lymphocytes subsets, multiple linear regression models were used. The coefficient of determination (absolute values of r or ρ) was calculated as a measure of effect size: <0.140 is considered a small effect size, between 0.140 and 0.361 is a medium effect size and >0.361 a large effect size (Kotrlik & Williams 2003).

Overall, differences were considered statistically significant for p-values below 0.05. The results were analyzed using IBM SPSS Statistics version 23 (IBM Corporation, Armonk, NY, USA) and GraphPad Prism version 6 (GraphPad Software, La Jolla, CA, USA).

4. RESULTS AND DISCUSSION

4.1. Protocols' Optimization

The evaluation of thymic function and of immune system aging was preceded by a period of optimization of techniques that were not performed in our laboratory previously. A substantial part of this thesis technical work consisted in the optimization of the Flow-FISH for length of telomere repeats evaluation and Nested-PCR for TRECs quantification. In this section, we describe the major optimization steps performed to optimize these techniques.

4.1.1. Flow-FISH Protocol Optimization for Quantification of Tength of Telomere Repeats

As flow cytometry permits a multiparametric evaluation, Flow-FISH constitutes a very powerful tool to determine the hybridization of a specific probe to different cell subsets. The first step on the optimization of this technique was to test whether we could promote the binding of the PNA probe to a mix of bovine thymocytes and human PBMCs accordingly to the protocol described by Baerlocher *et al.* (Baerlocher et al., 2006).

The results obtained showed that the PNA probe was internalized and hybridized as expected, showing up in 2 peaks (**Figure 5.**). Each of the peaks should correspond to the two cell subsets, mixed in a single tube, containing different length of telomere repeats and reflected on different PNA hybridization. Based on the fact the bovine thymocytes have 2-3 longer telomeres in comparison to human PBMCs (Baerlocher et al., 2006), one could infer that the peak with the higher PNA mean fluorescence intensity (MFI) should correspond to bovine thymocytes, and the other to human PBMCs. To confirm this, we repeated the assay by adding LDS751.

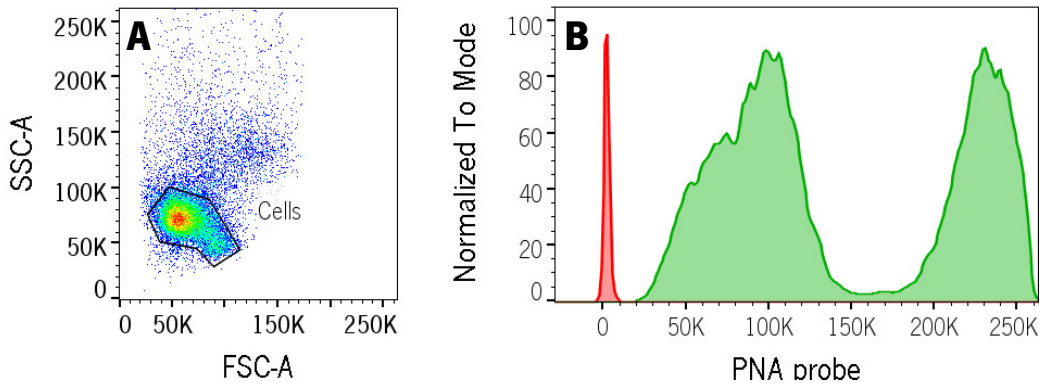

Figure 5. PNA probe hybridization in a mixture of bovine thymocytes and human PBMCs. A. The cells were selected in accordance to size (FSC-A) and complexity (SSC-A). **B.** The PNA hybridized as expected and two peaks corresponding to the human PBMCs and bovine thymocytes were evident (green histogram). Accordingly to Baerlocher *et al.* the peak on the far right should correspond to bovine thymocytes as they contain longer telomers (Baerlocher et al., 2006). A control without PNA probe was included (red histogram).

LDS751 is a DNA fluorescent dye (LDS751) capable of entering all cells and counterstain them. Because the fixation process hampers the internalization of LDS751, and bovine thymocytes were mildly fixed during their preparation, it was expected for these cells to present lower LDS751 MFI in comparison to the human PBMCs, that were used fresh. Results showed that cells with the higher PNA MFI were, as expected, bovine thymocytes as they had lower LDS751 MFI and that human PBMCs had the shorter telomeres, as they presented decrease PNA MFI and were brighter for LDS751 (**Figure 6.**).

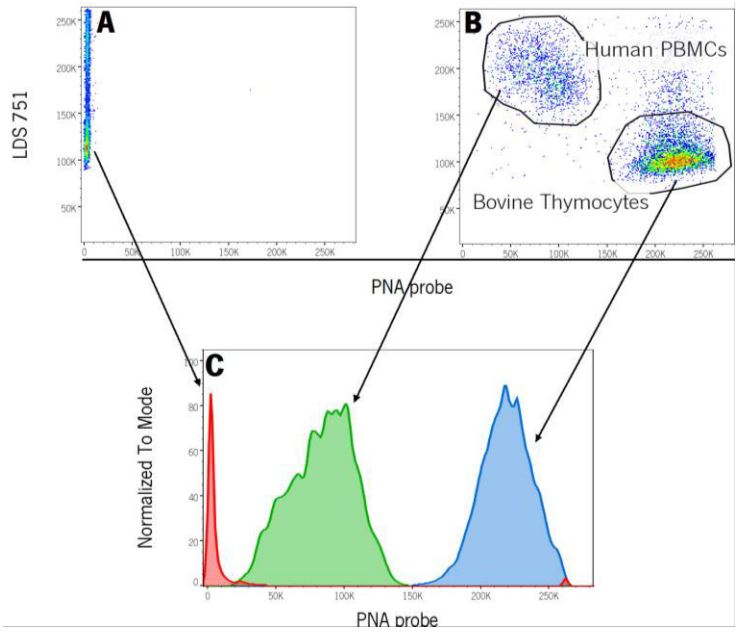

Figure 6. PNA probe hybridization and counterstaining with the DNA dye LDS751 on human PBMCs and bovine thymocytes. Cells were incubated with LDS751 in the absence (**A**) or presence of the PNA probe (**B**). Human PBMCs showed higher LDS751 internalization (**B**) and lower PNA probe hybridization (**C**) while the bovine thymocytes showed lower LDS751 internalization (**B**) and higher PNA probe hybridization (**C**)

As we aimed to quantify the relative length of telomere repeats of specific PBMC cell subsets (namely $CD4^+$ and $CD8^+$ T lymphocytes) in individuals with different MS progression forms, we then proceeded to the optimization of antibody surface stain to identify each of those populations. As many reports claim that antibody stain is a major difficulty of the technique since the harsh conditions of the protocol affect the fluorochromes, the antibody and/or the epitope (Baerlocher et al., 2006; Montpetit et al., 2014), we tested a broad set of antibody clones coupled to different fluorochromes. Each antibody was tested independently in a tube and surface stain was performed before or after the hybridization protocol (though the PNA probe itself was not included); as a reference, we performed a conventional PBMC surface stain (as described in **section 3.3; Figure 7.**). The results obtained showed that the hybridization protocol performed after antibody incubation hampered the detection of the all the antibodies tested. We hypothesized that fluorochromes were not able to support the harsh conditions of the hybridization protocol, such as the achieved high temperatures.

In what regards the surface stain after the hybridization protocol, we observed that, apparently, all the antibodies tested were detected although with lower fluorescence intensity comparing to the stain without the hybridization protocol (**Figure 7.**). As for the CD3, CD4 and CD8 markers the negative population was not evident, we hypothesized that the fluorescence detected could be a result from unspecific binding of the antibodies. Therefore, we performed another experiment using the hybridization protocol and performing a blockage of the Fc receptors with human serum (10% in PBS) before incubation of the antibodies. After Fc receptor blockage, we observed that the signal detected after hybridization for CD3, CD4 and CD8 markers was lost while the signal for CD45 was maintained for both fluorophores, suggesting that apart from CD45 the fluorescence detected for the remaing markers was probably due to unspecific binding.

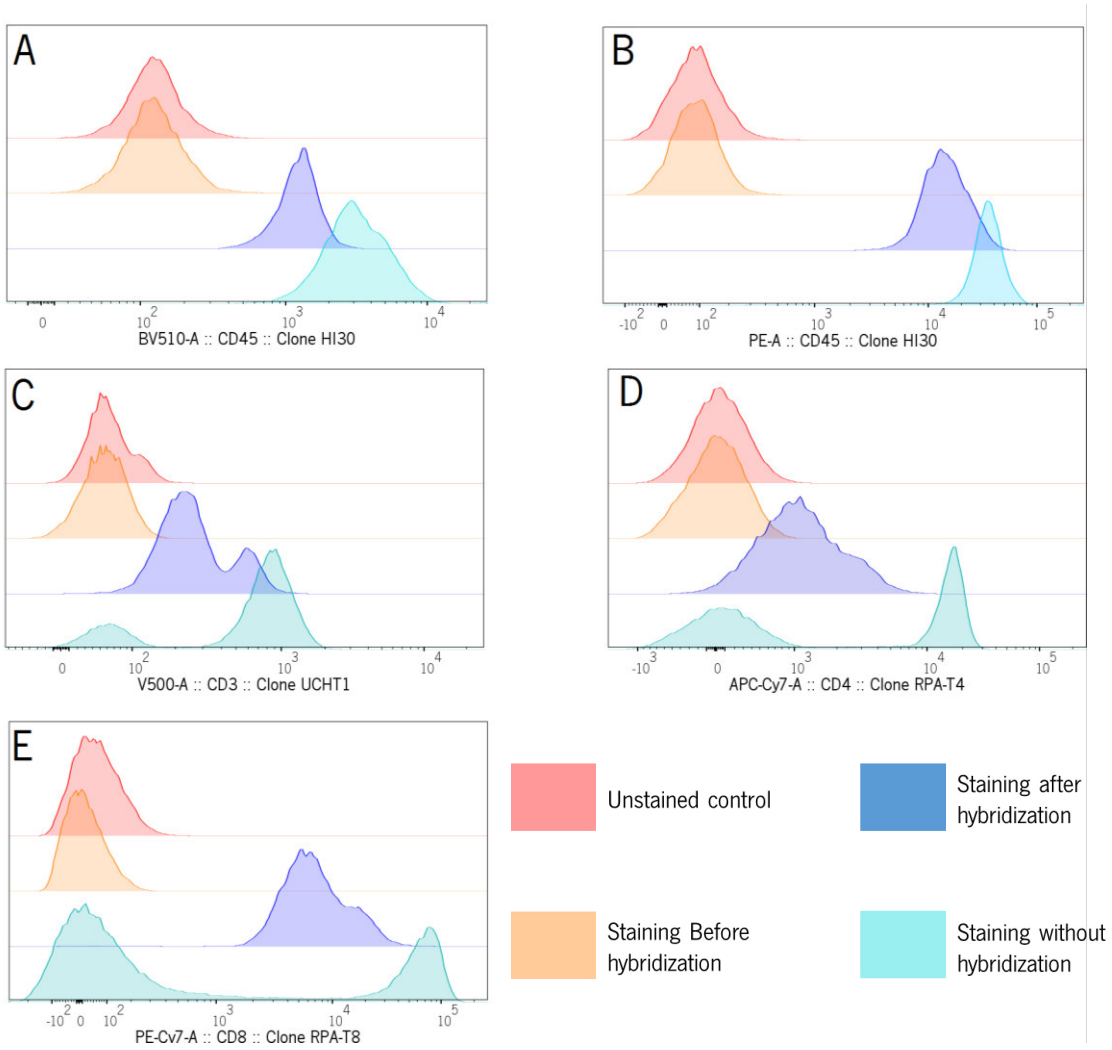

Figure 7. Surface stain of human PBMCs before and after hybridization. A, **B**, **C**, **D** and **E**, correspond to the surface staining of the BV510-conjugated anti-CD45 clone HI30, PE-conjugated anti-CD45 clone HI30, V500-conjugated anti-CD3 clone UCHT1, APC-Cy7-conjugated anti-CD4 clone RPA-T4 and Pe-Cy7-conjugated anti-CD8 clone RPA-T8 respectively. As reference, stained samples that were not submitted to the hybridization protocol were included. When performing the hybridization protocol, the markers were only detected when the antibody stain was performed after the hybridization protocol, with slight decrease on the fluorescence intensity in comparison to samples that were not submitted to the hybridization protocol.

Results so far suggested that: i) the hybridization protocol destroys all the fluorochromes tested (i.e. BV510, V500, Pe, Pe-Cy7 and APC-Cy7); ii) hybridization leads to the denaturation of the CD4 and CD3 epitopes being detect by the antibodies but not of the CD45 epitopes. For these reasons, for CD4 and CD3 detection, we adopted another strategy and used a biotinylated anti-human CD3 and a rat-purified anti-human CD4 before performing the hybridization protocol; afterwards, cells were incubated with pacific blue-conjugated streptavidin and a PE-conjugated goat anti-rat antibody (secondary); all this procedure was performed after Fc receptors blockage with human serum. With this approach, we

guaranteed epitope detection before hybridization, revealed posteriorly upon incubation with a fluorescent polyclonal anti-rabbit or streptavidin. The results obtained showed that this approach was equivalent to the incubation only with streptavidin or goat anti-rat only (**Figure 8.**). We hypothesized that, although Fc receptors blockage, the harsh conditions of the protocol could be altering the variable portion of the primary antibody, leading to the unspecific binding of the secondary antibody and of the streptavidin, avoiding their detection; alternatively, the hybridization protocol could be detaching the antibodies from their epitopes.

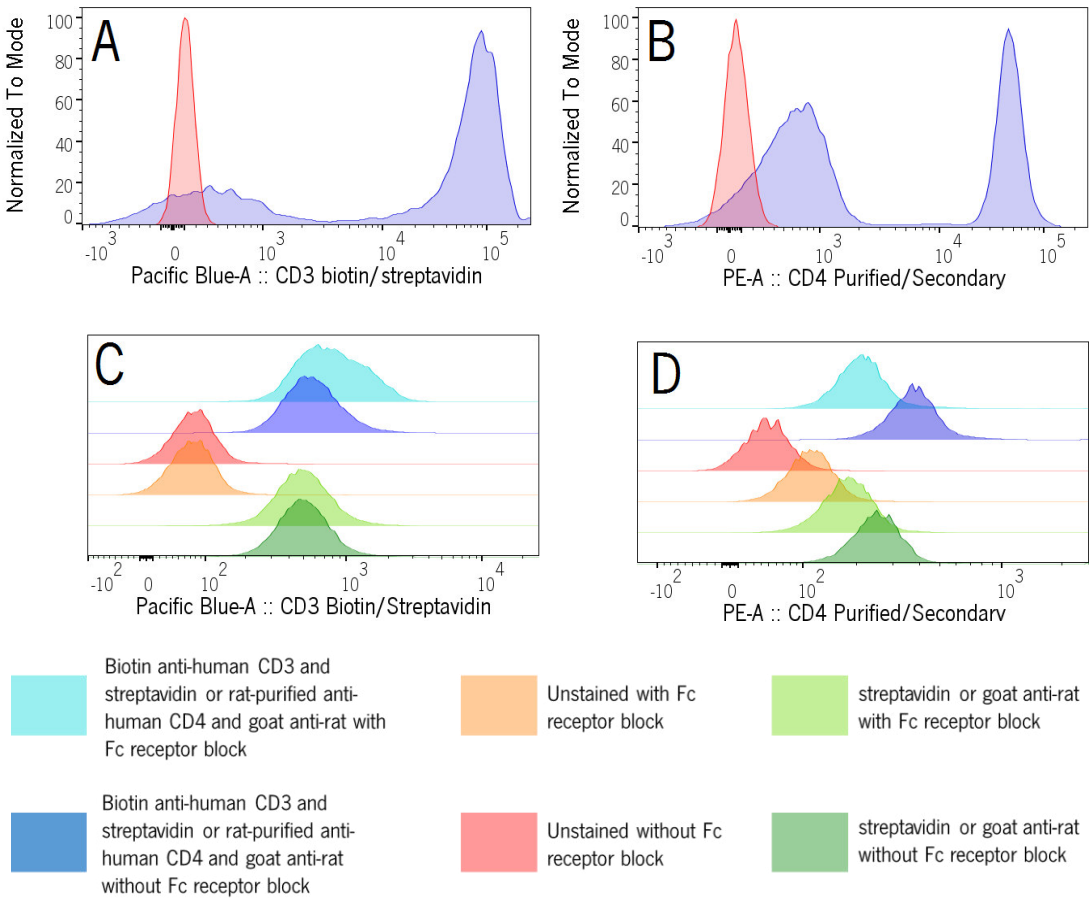

Figure 8. Surface staining of human PBMCs using the biotin anti-human CD3/streptavidin and rat-purified anti-human CD4/goat anti-rat antibodies. Incubation of the human PBMCs with the biotin anti-human CD3 and pacific blue-conjugated streptavidin anti-biotin and rat-purified anti-human CD4 and a PE-conjugated goat anti-rat antibody without vs. upon hybridization (**A** vs. **C** and **B** vs. **D**, respectively). The incubation of both antibodies for the CD3 or CD4 were detected similarly to the streptavidin or goat anti-rat only.

To overcome the possible detachment of the antibody to its cognate antigen and the unspecific binding of the secondary protein/antibody we performed a fixation step after incubation with the purified and biotinylated antibodies and before the hybridization protocol; this fixation was performed using a fixation/permeabilization kit (Foxp3 Staining buffer set; eBioscience). We hypothesized that fixation would permit the binding of the antibody to its cognate antigen and concomitantly permeabilization would allow PNA probe internalization. With this strategy, we could clearly distinguish the $CD3^+$ and $CD4^+$ populations (data not shown).

We then tested the full stain using the following sequences of step: i) incubation with rat-purified anti-human CD4 and biotinylated anti-human CD3; ii) fixation and permeabilization; iii) hybridization of the PNA probe; iv) incubation with BV510-conjugated anti-human CD45, PE-conjugated anti-rat and pacific blue-conjugated streptavidin; v) incubation with LDS751. From the results obtained we found that the population with decreased internalization of LDS751 (bovine thymocytes) did not expressed CD45 contrarily to the human PBMCs as expected (**Figure 9. A**). As we could distinguish the human PBMCs from the bovine thymocytes based only on the anti-human CD45, we abolished the use of the LDS751 from our protocol (**Figure 9. B**). Regarding the CD3 and CD4 stain within $CD45^+$ cells (human PBMCs) we could detect the $CD4^+$ T lymphocytes ($CD3^+CD4^+$) and considered the $CD3^+CD4^-$ as $CD8^+$ T lymphocytes (**Figure 9. C**). Regarding the detection of the PNA probe, we noticed that the signal was very variable between samples (**Figure 9. D**). This artifact could be related with the fact that the fixation and permeabilization reagents could enter the cells and promote fixation of the intracellular proteins, including the histones associated to the DNA; this would hamper the decondensation of the DNA strand and prevent the binding of the PNA probe to the telomere repeats.

The following step consisted on the fixation of the biotin anti-human CD3 and rat-purified anti-human CD4 with BS_3, a reagent able to fix the cell surface proteins but unable to enter the cell. Following the protocol described in **section 3.4.2.**, the results obtained showed that the BS_3 allowed the surface staining of the cells of interest without compromising the hybridization of the PNA probe to the telomere repeats (**Figure 10.**). This protocol also yielded less variability on the PNA probe MFI between replicates (**Figure 10. D** and **E**).

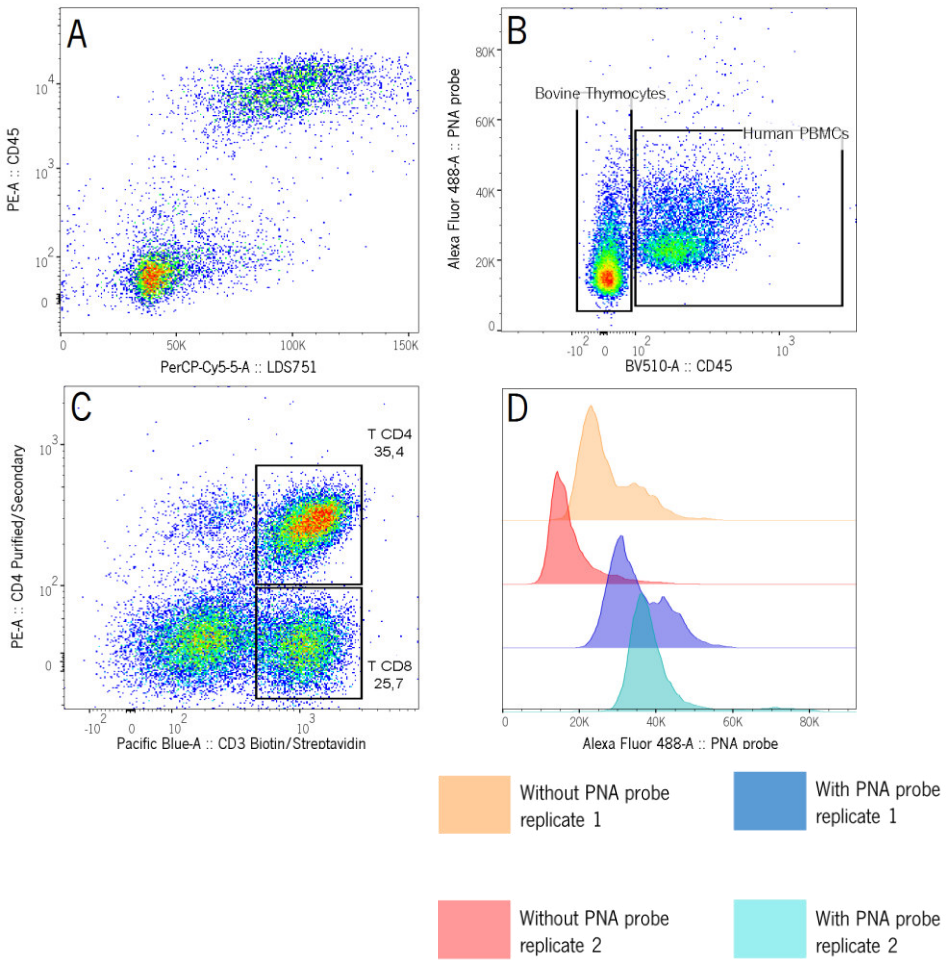

Figure 9. Cell surface staining and PNA probe hybridization after fixation and permeabilization of the cell membrane. Cells presenting lower LDS751 internalization (bovine thymocytes) lack expression of CD45 cell surface marker **(A)** which allows the separation of bovine thymocytes from human PBMCs **(B).** Within the human PBMCs, the use of the fixation and permeabilization solution allows the detection and separation of $CD4^+$ from $CD8^+$ T lymphocytes through detection of CD4 and CD3 surface markers **(C).** In $CD4^+$ T lymphocytes, the signal of fluorescence detected from the PNA probe after fixation and permeabilization is extremely variable.

In the context of this MSc project, we could fully optimize this technique. However, due to time constrains, we were not able to quantify T lymphocytes' relative length of telomere repeats on the samples from MS patients and healthy controls.

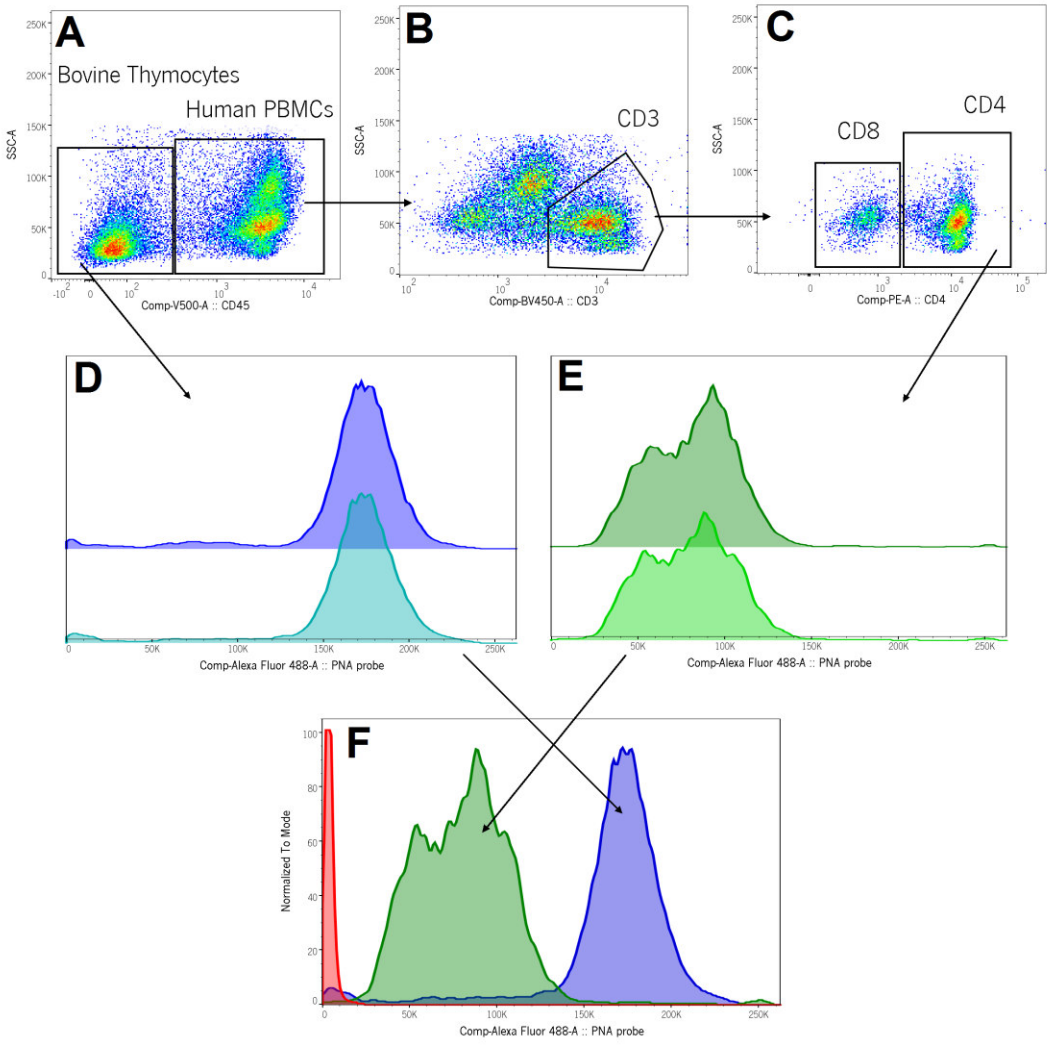

G

$$\text{Relative length of telomere repeats} = \frac{\text{MFI (human PBMCs) - MFI (negative control)}}{\text{MFI (bovine thymocytes) - MFI (negative control)}}$$

Figure 10. Gating strategy determination of the relative length of telomere repeats on bovine thymocytes and on CD4⁺ T lymphocytes subsets. Cell debris is initially excluded in accordance to its small size (FSC-A) and absence of the CD45 markers and within the gated-cells, singlets are selected (FSC-H *vs.* FSH-A plot), followed by gating of the cells based on their size and complexity (FSC-A *vs.* SSC-A plot; data not represented). Based on the expression or not of the CD45 marker the human PBMCs and the bovine thymocytes were gated, respectively (**A**). Within the human PBMCs, T lymphocytes were selected based on their expression of CD3 (**B**) and the subsets of CD4 and CD8 gated within this population (**C**). The histograms of the PNA probe of the bovine thymocytes (**D**) and CD4⁺ (**E**) were obtained and overlaid with the negative control without the PNA probe incubation (**F**). The length of telomere repeats of the T lymphocytes subsets is then calculated relatively to the bovine thymocytes using as reference in the negative control (**G**). MFI, mean fluorescence intensity.

4.1.2. Nested-PCR Protocol Optimization for TRECs Quantification

TREC containing T lymphocytes are extremely rare in the peripheral blood. For that reason, its quantification requires extremelly sensitive techniques such as Nested-PCR where the amplicons from a conventional PCR are amplified by quantitative PCR (qPCR). This approach for TREC quantification was described by Dion *et al.* (M. Dion et al., 2007) and was optimized in the laboratoty in our context of this MSc project.

We started this protocol optimization by testing the amplifications of the housekeeping gene CD3γ and of the sjTREC contained on the plasmid (provided by R. Cheynier, Institute Cochin, Paris, France) were occurring. The results obtained showed that both sequences within the plasmid were being amplified (**Figure 11. A**). Regarding the no-template controls for both PCRs, no major concerns were found since the amplification observed was probably due to primer dimer as observed from the melting curve (**Figure 11. B**).

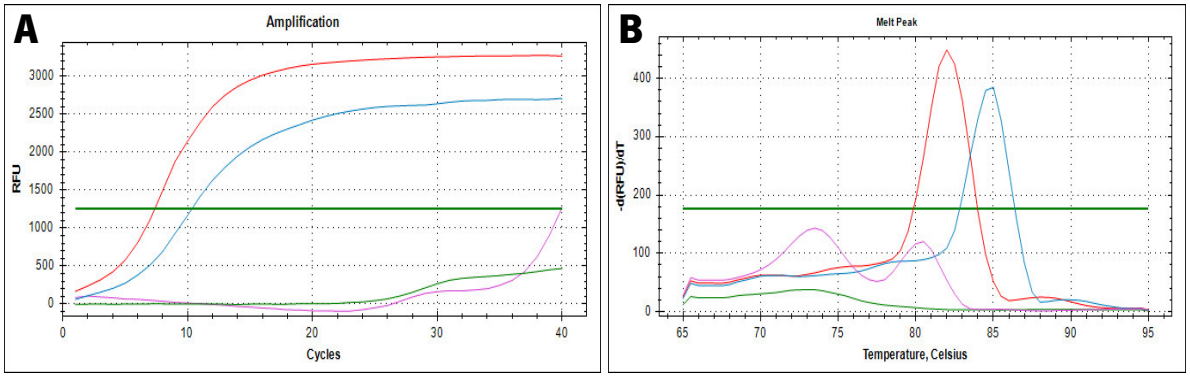

Figure 11. Amplification of sjTRECs and CD3γ from the plasmid by Nested-PCR. A. Amplification curves of CD3γ, sjTRECs and respective negative controls (with PCR grade water). **B.** Melting curves obtained for the amplification. The red and the blue lines correspond to the amplification of the CD3γ and of the sjTREC sequences on the plasmid, respectively. The green and the purple lines correspond to the CD3 and sjTREC negative controls, respectively.

After confirming the amplification of both sequences on the plasmid, we then moved and construct a calibration curve for each sequence by performing 8 sequential 10-fold dilutions. Additionally, we tested the amplification on 2 distinct PBMC donors. Regarding the calibration curves, the results obtained showed that the gap between each of the dilutions was similar for both sequences, as expected (**Table 2.**). However, when amplifying the CD3γ or the sjTREC primers on the same dilutions of plasmid, the Cq values were not concordant. These results were not anticipated as the

plasmid contained a single copy from each sequence and, for that reason, for the same plasmid dilutions one would expect the CD3γ and the sjTREC amplification to have similar Cq values.

Table 2. Cq values of the CD3γ and sjTREC calibration curves. Calibration curves we obtained from eight 10-fold dilutions of the plasmid's amplicons from the conventional PCR, starting at 10^5 plasmid copies/μL.

Plasmid starting concentration	CD3γ		sjTREC		ΔCq sjTREC-CD3 [c]
(copies/μL)	Cq [a]	ΔCq [b]	Cq [a]	ΔCq [b]	
10^5	na		na		
10^4	5.35	-	13.36±0.18	-	8.01
10^3	9.45±0.26	4.10	16.93±0.10	3.57	7.48
10^2	13.12±0.03	3.67	20.25±0.10	3.32	7.13
10^1	16.65±0.25	3.53	23.34±0.12	3.08	6.68
10^0	20.29±0.08	3.63	26.84±0.06	3.50	6.55
10^{-1}	23.55±0.27	3.26	29.42±0.04	2.58	5.87
10^{-2}	26.93±0.35	3.39	32.73±0.63	3.32	5.80
r^2	0.999		0.998		
Slope [d]	3.539		3.200		
Efficiency (%) [e]	91.7		105.4		

[a] Cq values are represented as the mean ± standard deviation from duplicates. Whenever, from some reason, only one of the duplicates was available, no standard deviation is represented;
[b] Cq difference between two consecutive plasmid dilutions;
[c] Cq difference between the two genes, for the same dilution;
[d] Slopes were obtained from the representation of Cq *vs.* log (plasmid starting concentration);
[e] qPCR efficiency calculated based on the formula: e = (10(−1/Slope) − 1) x 100.
Cq, Quantification cycle
na, no amplification

Regarding the amplification of sjTREC and CD3γ in human samples, from the results obtained we observed that the sjTRECs concentration in the human samples was too high relatively to the CD3γ quantification (**Table 3.**). We expected around 10^0-10^3 TRECs and 10^4-10^5 CD3γ copies per 10^5 PBMCs (Geenen et al., 2003; Poulin et al., 2012). However, our results showed that sjTRECs were being amplified very early and in a magnitude comparable to CD3γ. Because the qPCR is based on the product of the conventional PCR, if the number of amplification cycles being used on the conventional PCR sets the amplification products on the plateau and not on the exponential phase, this could lead to the over-quantification of sjTREC, relative to CD3γ. Based on this, we expected that fewer amplification cycles on the conventional PCR could lead to more reliable results in what concerns to the concentration of TRECs on the human samples.

Table 3. Quantification of the starting quantity of CD3γ and sjTRECs sequences in human PBMC samples.

Sample	Sequence	Cq [a)]	Starting concentration (copies/μL) [b)]
Donor 1	sjTREC	12.54±1.62	(7.6±6.3) x10^4
	CD3	7.39±0.48	(8.7±2.5) x10^4
Donor 2	sjTREC	12.76±1.06	(5.9±3.5) x10^4
	CD3	7.61±0.69	(7.8±3.2) x10^4

[a)] Cq values are represented as the mean ± standard deviation from duplicates. Whenever, from some reason, only one of the duplicates was available, no standard deviation is represented;
[b)] Calculation on the starting concentration was performed based on the calibration curve from **Table 2**.
Cq, Quantification cycle

Upon decreasing the number of amplification cycles on the conventional PCR from 22 to 18 or 19, results showed that the quantification cycle (Cq) difference for the amplification of sjTRECs and CD3γ after 19 amplification cycles was around 4 cycles, while with 18 amplification cycles that difference was around 7 to 9 cycles (**Table 4.**). However, it was not possible to determine the absolute amount of CD3γ and sjTREC, as no calibration curve was made on this assay. Because of this increase on the Cq difference, we used on the following assays 18 cycles of amplification on the conventional PCR.

Table 4. Optimization of the number of amplification cycles on the conventional PCR.

Sample	Amplification cycles on conventional PCR	Cq_{CD3}	Cq_{sjTREC}	$\Delta Cq_{sjTREC-CD3}$
Donor 1	19	11.07± 0.11	15.26±0.47	4.19
	18	13.18±0.23	19.89±0.15	6.71
Donor 2	19	11.35±0.10	16.02*	4.67
	18	12.42±0.26	21.41±0.07	8.99

Cq, Quantification cycle

Additionally, to the over-quantification of the sjTREC sequence in comparison to the CD3γ on the human PBMC samples, we also observed that the calibration curves of both sequences were not overlapping (**Table 2;** this would be expected since the plasmid contains one copy from each sequence). As the efficiency of the qPCR for both sequences amplification was on the expected range (*i.e.* 90 to 100%), we assumed that the qPCR was properly optimized and the issue would be on the conventional PCR. To improve the conventional PCR, we tested plasmid amplification using different

annealing temperatures ranging from 58°C to 62°C, being 60°C the temperature being used up until now. After the conventional PCR, amplicons were quantified by qPCR. From the results obtained we concluded that the annealing temperature on the conventional PCR was not preponderant since the Cq remain discordant for both sequences on the same plasmid dilutions and for that reason we decided to keep the 60°C (**Table 5**).

Table 5. Melting temperature optimization of the conventional PCR.

Conventional PCR Annealing temperature	Starting concentration (copies/µL)	$Cq_{CD3\gamma}$	Cq_{sjTREC}	$\Delta Cq_{sjTREC-CD3}$
62°C	10^4	18.69	22.50	**3.81**
	10^3	16.35	20.07	**3.72**
61°C	10^4	16.20	20.24	**4.04**
	10^3	13.19	18.61	**5.42**
60°C	10^4	17.03	21.27	**4.24**
	10^3	14.39	19.10	**4.71**
59°C	10^4	21.37	21.77	**0.40**
	10^3	12.14	18.53	**6.39**
58°C	10^4	24.84	na	-
	10^3	12.96	18.66	**5.7**

a) Cq values; only 1 replicate for each dilution was performed.
Cq, Quantification cycle;
na, no aplification

Currently, we are studying which factors might be contributing to the lack of overlap of the calibration curves for sjTREC and CD3γ so we can overcome this issue and proceed to TREC quantification on samples from MS patients and healthy controls.

4.1.3. Blood Cells Phenotypical Analysis

The use of labeled-antibodies allowed us the determination and phenotypic analysis of the different cell subsets. No major drawbacks were found since the flow-cytometry technique and analysis was already optimized on the laboratory. For the determination of different cell subsets, it was necessary to titrate a panel of antibodies accordingly and the gating strategy was defined as followed:

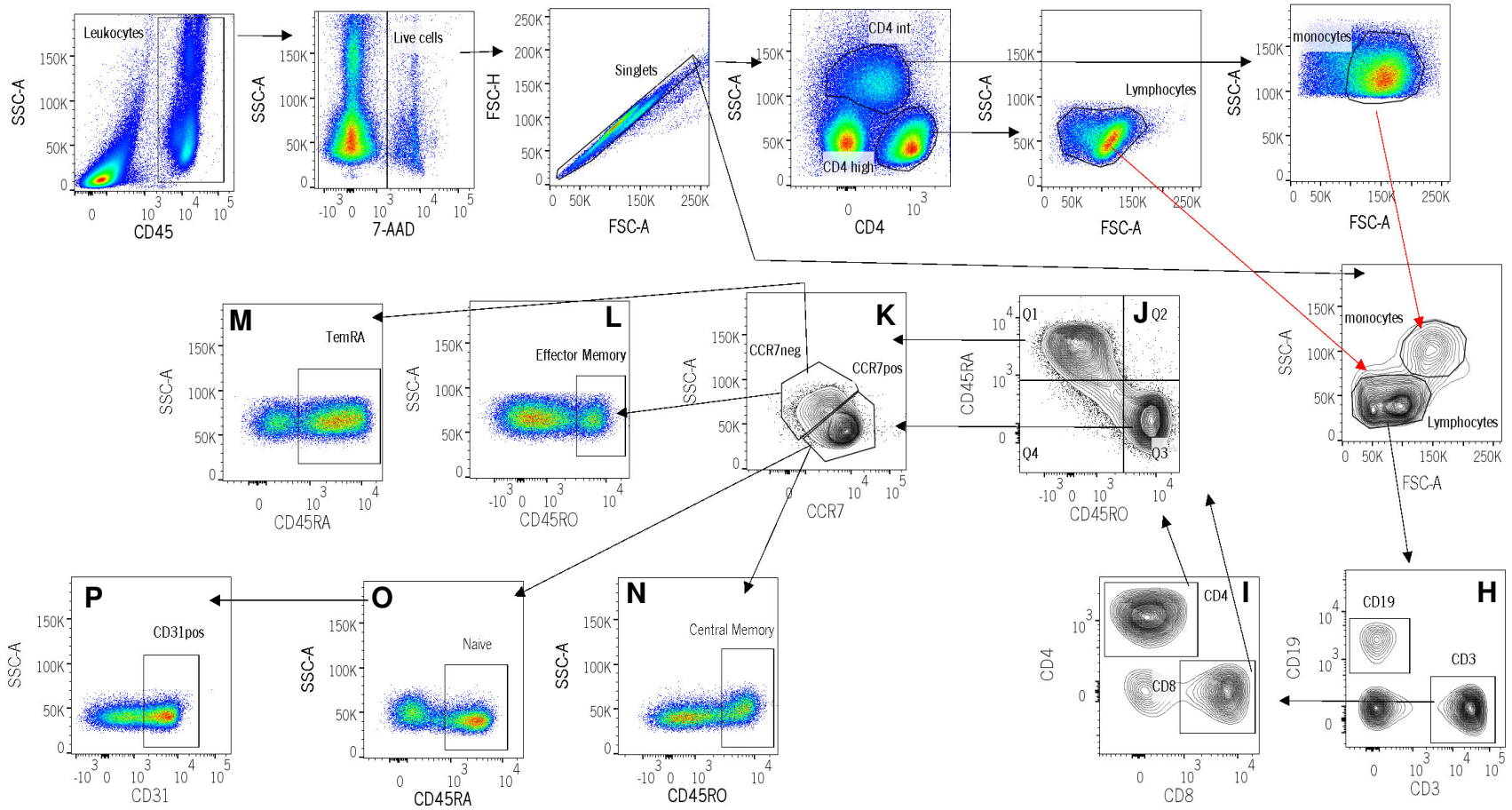

Figure 12. Gating strategy for phenotypical analysis of the T lymphocytes subsets. Leukocytes were selected by presence of CD45 cell marker. (**A**) and viable cells selected by exclusion of 7AAD positive cell subset (**B**). After isolating the singlets (**C**), the monocytes and lymphocytes were gated (**G**) regarding their expression of the CD4 marker and complexity (**D**; medium CD4 expression and medium side scatter [**E**] and high CD4 expression and low side scatter [**F**], respectively). $CD19^+$ B lymphocytes were then distinguished from $CD3^+$ T lymphocytes within the lymphocytes population (**H**). Using CD4 and CD8 markers helper T lymphocytes ($CD3^+CD4^+$) and cytotoxic T lymphocytes ($CD3^+CD8^+$) were distinguished and within each one of these populations (**I**). In accordance to the expression of the isoform of CD45 (RA or RO; **J**) and presence or absence of CCR7 (**K**), Effector Memory ($CD45RA^-CD45RO^+CCR7^-$; **L**), Effector Memory with expression of the RA isoform of the CD45 marker ($CD45RA^+CD45RO^+CCR7^-$; **M**), Central Memory ($CD45RA^-CD45RO^+CCR7^+$; **N**) and Naïve ($CD45RA^+CD45RO^-CCR7^+$; **O**) were isolated. Finally, recent thymic emigrants were defined within the naïve population by the expression of the CD31 marker ($CD45RA^+CD45RO^-CCR7^+CD31^+$; **P**). Red arrows correspond to backgating of monocytes and lymphocyte

4.2. Evaluation of the thymic function and of the immune system aging in individuals with distinct multiple sclerosis progression forms

To study how thymic function and immune system aging correlate in MS patients with distinct forms of progression of the disease we decided to evaluate several T lymphocytes subsets. Although these cells have been related to the pathophysiology (Duszczyszyn et al. 2006; Fletcher et al. 2010), of the disease data regarding the comparison between the distinct forms of progression is lacking. We determined the percentage of RTE, naïve, CM, EM and TEMRA on CD4+ and CD8+ T lymphocytes. The percentage of these cell subsets provide an estimation of thymic function and of immune system aging since, as thymus involutes with age, the production of RTEs is impaired, and consequently the peripheral seeding is also decreased, which leads to the decrement of naïve cells, and to the increased percentage of memory cells (Simon, Hollander, and McMichael 2015; Sprent and Surh 2011).

4.2.1. Correlation Between T Lymphocytes Subsets and Age on Patients with Different Multiple Sclerosis Progression Forms and Healthy Individuals

As thymic function and immune system aging surrogates are variables that vary greatly with age (Lynch et al., 2009; Saule et al., 2006) we started by correlating each of the evaluated cell subsets with age, stratifying individuals accordingly to their MS progression form (RRMS or PPMS), and compared those with the correlations on the healthy controls. We determined whether the T lymphocytes and its main subsets, namely $CD4^+$ and $CD8^+$ T lymphocytes percentages, correlated with age. We observed that the negative correlation of age with T lymphocytes on healthy individuals had a large effect size ($|r| = 0.5164$), as opposed to what was observed for RRMS and PPMS patients, where no correlation was observed at all (**Figure 13. A**). Moreover, for the $CD4^+$ and $CD8^+$ T lymphocytes and their ratio, neither the healthy individuals nor the RRMS or PPMS patients presented significant correlations with age (**Figure 13. B, C** and **D**).

Regarding the CD4+ T lymphocytes subsets, a significant negative correlation with a large effect size ($|r| = 0.4427$) was found on healthy individuals for RTEs CD4+ T lymphocytes' percentages with age, as expected (Junge et al. 2007). This correlation was not significant neither for RRMS nor for PPMS patients though, the former nearly achieved significan negative correlation with a large effect size ($p=0.0633$, $|r| = 0.4464$) (Figure 18. A). Furthermore, no significant correlations were found between

age and naïve, CM EM or TEMRA CD4+ T lymphocytes for any of the groups studied (**Figure 14. B**, **C**, **D** and **E**). Concerning the naïve to memory CD4⁺ T lymphocytes' ratio, only healthy individuals presented significant negative correlations, with a large effect size (|r| = 0.4041) (**Figure 14. F**).

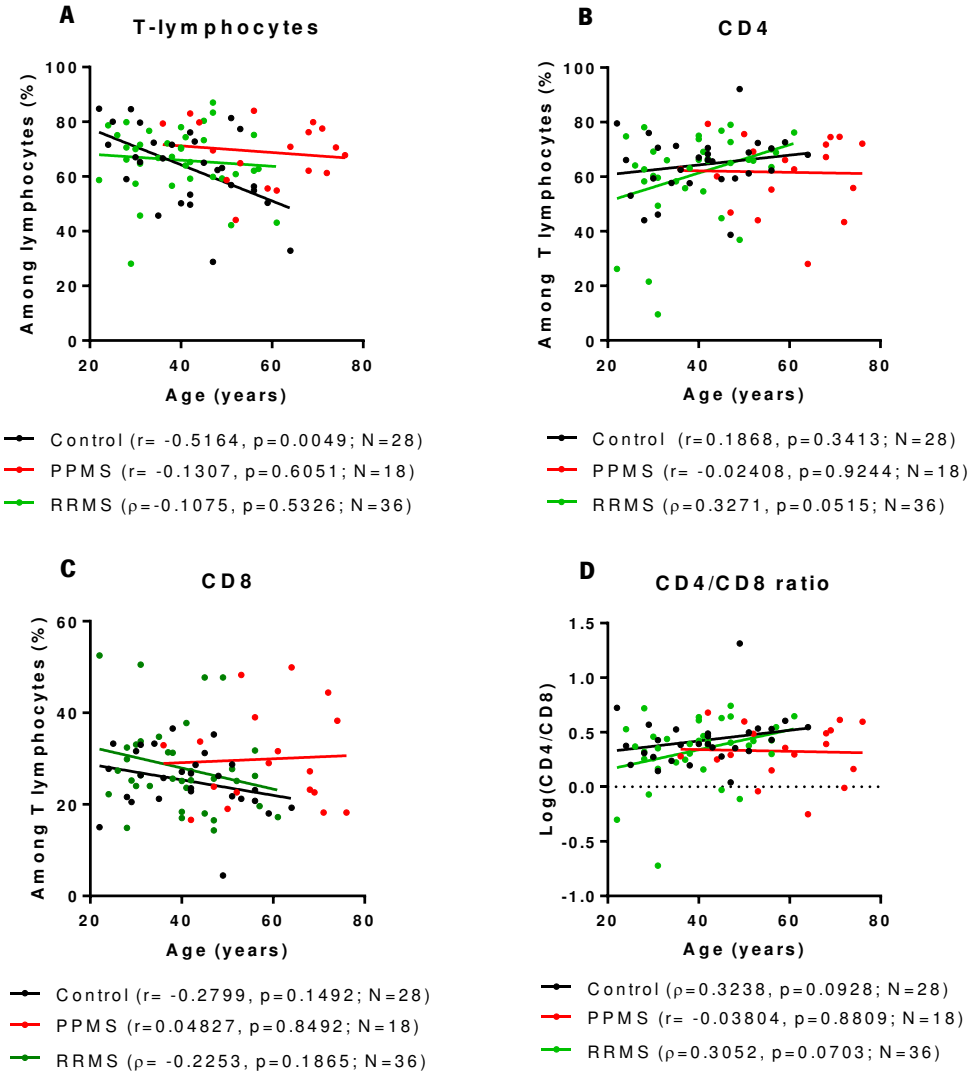

Figure 13. Correlation between percentage of T lymphocytes subsets with age for healthy individuals and for RRMS and PPMS patients. Represented are the T lymphocytes (**A**), CD4⁺ T lymphocytes (**B**), CD8⁺ T lymphocytes (**C**), and CD4⁺/CD8⁺ T lymphocytes ratio (**D**). Each dot represents one individual and the line the correlation between the 2 variables; black line and dots correspond to healthy individuals; red line and dots correspond to PPMS patients; and green line and dots correspond to RRMS patients. Correlations were determined using Pearson correlation coefficient (r) or Spearman's rank correlation coefficient (ρ) in accordance to the normal or non-normal distribution of variables, respectively. p, p-value (statistically significant when <0.05); N, sample size.

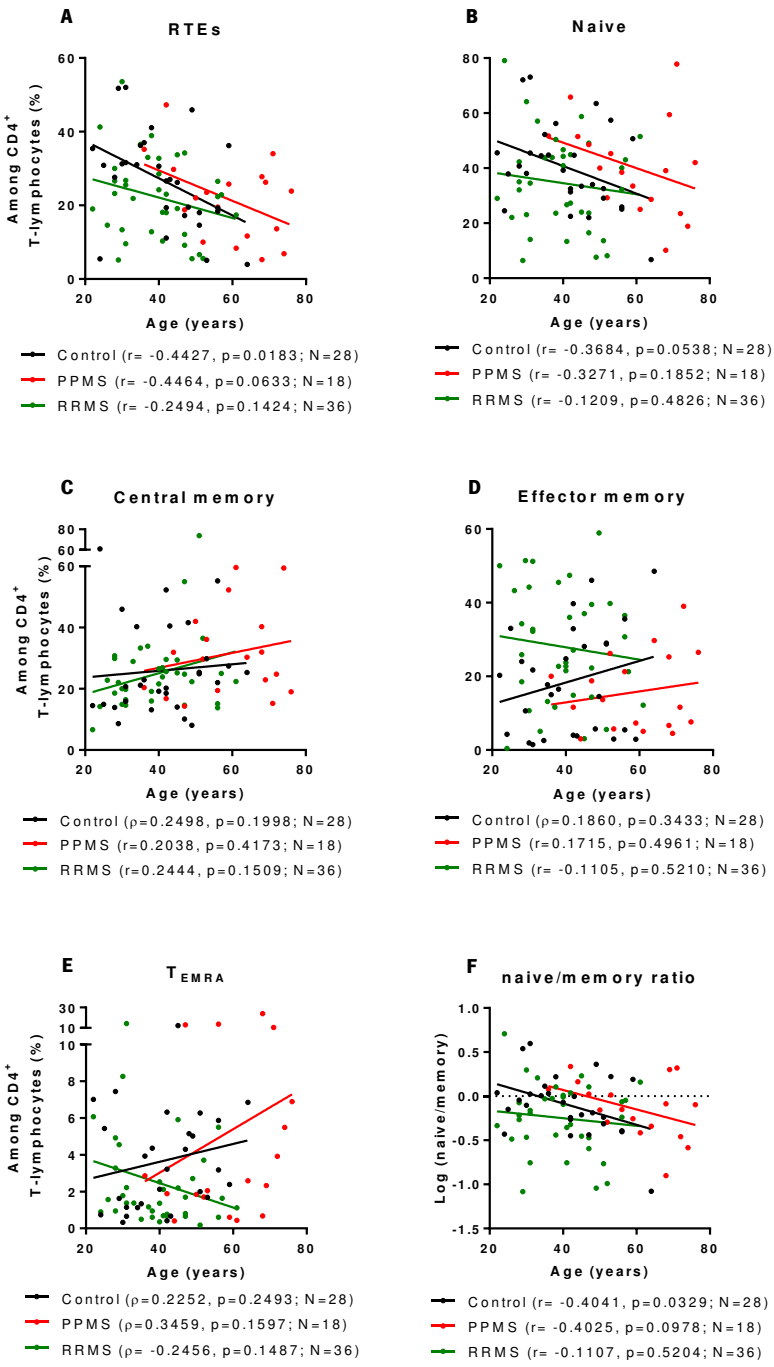

Figure 14. Correlation between percentage of CD4⁺ T lymphocytes subsets with age for healthy individuals and for RRMS and PPMS patients. Represented are the RTEs (**A**), naïve (**B**), central memory (CM; **C**), effector memory (EM; **D**), and T_{EMRA} (**E**) $CD4^+$T lymphocytes. The naïve to memory $CD4^+$T lymphocytes' ratio (**F**) was calculated as the ratio of naïve over the sum of CM, EM and T_{EMRA} subsets. Each dot represents one individual and the line the correlation between the 2 variables; black line and dots correspond to healthy individuals; red line and dots correspond to PPMS patients; and green line and dots correspond to RRMS patients. Correlations were determined using Pearson correlation coefficient (r) or Spearman's rank correlation coefficient (ρ) in accordance to the normal or non-normal distribution of variables, respectively. p, p-value (statistically significant when <0.05); N, sample size.

Regarding the CD8+ T lymphocytes subsets, a negative correlation, with a large effect size, was observed for RTEs and naïve cells percentages with age on healthy individuals (**Figure 15. A** and **B**); although only nearly significant, the same was observed for PPMS patients with similar values of effect size (p=0.0543 and $|\rho|$=0.4607 for RTE and p=0.0562 and $|\rho|$= 0.4576 for naïve cells). This was not observed for the RRMS patients; instead we verified that the correlation of age with RTEs and naïve CD8+ T lymphocytes was not significant and had a medium effect size. Regarding the memory CD8+ T lymphocytes subsets, a positive correlation was observed for CM with age on the healthy controls and for EM with age for the RRMS patients (**Figure 15. C** and **D**). No significant correlations were found on TEMRA CD8+ T lymphocytes percentages with age (**Figure 15. E**). Regarding the naïve to memory CD8+ T lymphocytes ratio we observed a significant negative correlation with age for PPMS patients but not for the other groups (**Figure 15. F**).

On general, the group presenting more significant correlations between age and the several T lymphocytes subsets was the one comprising the healthy individuals. In healthy individuals, negative correlations were found mainly for RTEs and naïve T lymphocytes subsets and positive correlations were found mainly on memory T lymphocytes subsets. These results were expectable as with age the immune system undergoes natural aging characterized by thymic involution and consequent decrease of thymic output leading to a decreased naïve to memory ratio (Briceño et al. 2016; Nikolich-Žugich 2014; Saule et al. 2006; Simon, Hollander, and McMichael 2015). Most of the correlations observed for healthy individuals were also present on PPMS individuals, though in some situations those correlations were only nearly statistical significant; however, as the correlations effect size were very similar between healthy and PPMS individuals, this suggests that increasing sample size would be enough to achieve significance. Interestingly, while the negative correlation between age and RTEs (both among CD4+ and CD8+ T lymphocytes) is significant or nearly significant on healthy and PPMS individuals respectively, this was not the case for RRMS individuals. This was also the case for the naïve to memory ratio on CD4+ and CD8+ T lymphocytes. Altogether, these results suggest an altered thymic function and an altered balance of the naïve and memory pool T lymphocytes on RRMS patients in comparison to controls and PPMS patients. These results are in accordance to other reports where individuals with RRMS present an increased immunological aging and decreased thymic function when compared with the age-matched healthy individuals (Balint et al. 2013; Duszczyszyn et al. 2006; Hug et al. 2003).

However, this is the first evidence for the fact that patients with PPMS are very similar to healthy individuals in what concerns to the evaluated parameters.

On overall, results showed that for many of correlations of the analyzed cell populations with age, RRMS patients stood out from PPMS and healthy individuals, presenting generalized different correlations and tendencies from the PPMS and control group. However, PPMS patients comprised older individuals in comparison to the other groups. Therefore, it is extremely relevant to control these analyses for these age differences. Furthermore, as most of the RRMS individuals were under therapy, we thought it would be relevant to evaluate how therapy could be contributing to the changes on T lymphocytes subsets percentages.

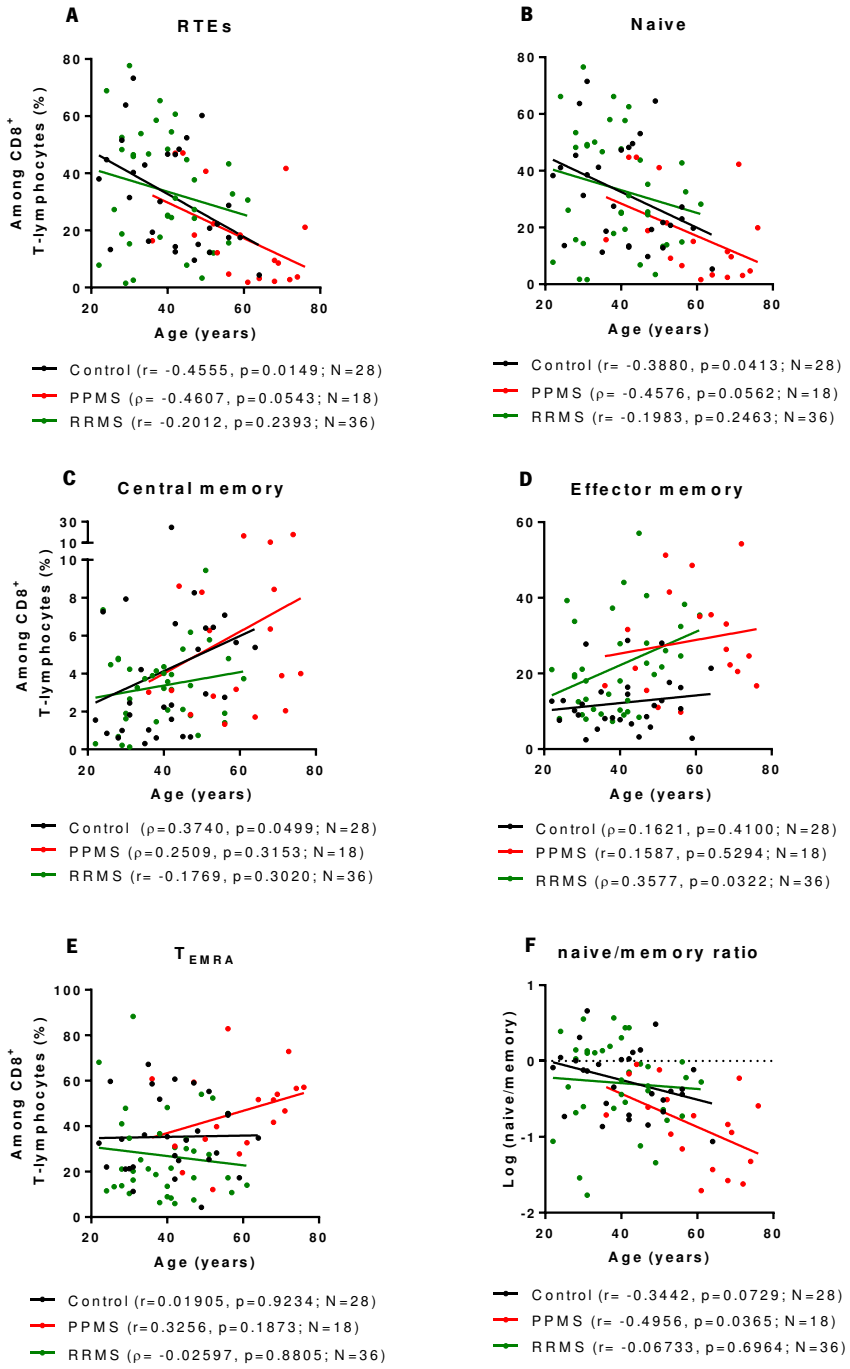

Figure 15. Correlation between percentage of CD8⁺ T lymphocytes subsets with age for healthy individuals and for RRMS and PPMS patients. Represented are the RTEs (**A**), naïve (**B**), central memory (CM; **C**), effector memory (EM; **D**), and T_{EMRA} (**E**) CD8⁺ T lymphocytes. The naïve to memory CD8⁺ T lymphocytes' ratio (**F**) was calculated as the ratio of naïve over the sum of CM, EM and T_{EMRA} subsets. Each dot represents one individual and the line the correlation between the 2 variables; black line and dots correspond to healthy individuals; red line and dots correspond to PPMS patients; and green line and dots correspond to RRMS patients. Correlations were determined using Pearson correlation coefficient (r) or Spearman's rank correlation coefficient (ρ) in accordance to the normal or non-normal distribution of variables, respectively. p, p-value (statistically significant when <0.05); N, sample size.

4.2.2. Age, Gender, Multiple Sclerosis Progression Form and Treatment as Predictors of Changes on the Percentages of T Lymphocytes Subsets

As several factors may contribute to the alterations on T lymphocytes subsets' percentages we decided to compute a multiple linear regression model to determine whether the differences observed in naïve and memory subsets may be predicted by age, gender, MS progression form and treatment. As for this research study a considerable set of T lymphocytes subsets were considered, we decided to determine for which subsets the linear regression model presented significant differences and further focus on those subsets.

Regarding $CD4^+$ T lymphocytes, the percentage of RTEs could be predicted by gender and age: men had less 6.270% RTEs in comparison to women and, per each year increased, a decrease of 0.336% RTEs was expected. These results may be related with the fact that men present lower thymic function than women due to hormonal factors (Pido-Lopez, Imami, & Aspinall, 2001). Interestingly, having RRMS or PPMS, in comparison to healthy controls did not had an impact on the percentage of RTEs $CD4^+$ T lymphocytes; the same was true for being or not on treatment (**Table 6.**). Regarding the predictor age on RTEs, the results were concordant with the natural and progressive thymic involution, which consequentely affects the exportation of these cells (Gui, Mustachio, Su, & Craig, 2012).

The naïve $CD4^+$ T lymphocytes were also affected by age. Addictionaly, results showed that individuals on treatment had 12.812% less naïve $CD4^+$ T lymphocytes in comparison to treatment naïve individuals. The percentage of EM $CD4^+$ T lymphocytes was also affected by treatment; individuals under treatment present, on average, 16.580% more of these cells than treatment naïve individuals. In the end, individuals under treatment had a naïve to memory ratio 0.902 Log lower than treatment naïve individuals (i.e., nearly 10-fold decrease; **Table 6.**).

Table 6. Multiple linear regression models to predict CD4⁺ T lymphocytes subsets percentages using as dependent variable gender, age, MS progression form (RRMS and PPMS) and treatment.

		CD4⁺ T Lymphocytes			
		% Recent thymic emigrants	% Naive	% Effector Memory	Log (Naive/Memory)
Gender [a)]	B	-6.270	-1.217	-2.033	-0.111
	SE	2.646	3.921	3.363	0.193
	β	-0.246	-0.035	-0.064	-0.063
	P	**0.020**	0.757	0.547	0.566
Age (years)	B	-0.336	-0.362	0.092	-0.017
	SE	0.111	0.164	0.141	0.008
	β	-0.382	-0.295	0.083	-0.273
	P	**0.003**	**0.030**	0.514	**0.040**
RRMS [b)]	B	0.574	5.296	-5.123	0.548
	SE	4.457	6.605	5.664	0.326
	β	0.024	0.160	-0.171	0.328
	P	0.898	0.425	0.369	0.097
PPMS [c)]	B	3.808	10.538	-8.746	0437
	SE	3.902	5.781	4.958	0.285
	β	0.133	0.266	-0.244	0.219
	P	0.332	0.072	0.082	0.129
Treatment [d)]	B	-6.000	-12.821	16.580	-0.902
	SE	4.034	5.978	5.126	0.295
	β	-0.252	-0.389	0.555	-0.542
	P	0.141	**0.035**	**0.002**	**0.003**
F(5,76)		5.271	2.644	4.694	3.473
$R^2_{adjusted}$		0.209	0.092	0.186	0.132
P-value		**0.000**	**0.029**	**0.001**	**0.007**

[a)] Reference category: female;
[b)] Reference category: healthy individuals and PPMS patients;
[c)] Reference category: healthy individuals and RRMS patients;
[d)] Reference category: treatment naïve.

Regarding the CD8⁺ T lymphocytes subsets, the models were significant for the prediction of the RTE, naïve and EM cells (**Table 7.**). The results show that age is a predictor for those variables, where per each year increase, a decrease of 0.552% and 0.495% of RTEs and naive CD8⁺ T lymphocytes was observed, respectively; on the contrary, per each year increase the percentage of EM CD8⁺ T lymphocytes increased by 0.231%. It is interesting to observe that neither the MS progression form nor treatment have an impact neither on the RTE nor on the naïve CD8⁺ T lymphocytes. However, for EM

$CD8^+$ T lymphocytes, PPMS patients present more 10.356% of these cells in comparison to healthy indiduals.

These results provide interesting data regarding the predictors contributing to the percentages of T lymphocytes subsets. Since it has been suggested that the alterations observed in the T lymphocytes subsets in MS patients were probably a cause/consequence of the disease (Dendrou et al., 2015; Khoury et al., 2000), we expected that the phenotype of the disease would be a predictor for percentage of several T lymphocytes subsets, which was not observed.

On averall, our results suggest that, among all the predictors considered, age and treatment are the variables that allow to predict most of the alterations observed for the T lymphocytes subsets. Moreover, apart from the EM $CD8^+$ T lymphocytes, the MS progression forms are not predictors for T lymphocytes subsets percentages alterations.

The results obtained for treatment, as a predictor of the T lymphocytes percentages seem concordant with the mechanism of action of several immunomodulatory drugs used to treat MS as most of them target mainly T lymphocytes subsets (Aktas, Küry, Kieseier, & Hartung, 2010; Rudick & Sandrock, 2004). The mechanisms of action of those drugs include sequestration of naïve cells on lymph nodes, restriction of EM T lymphocytes to enter the CNS, limitation of the cellular proliferation, among others (Aktas et al., 2010; Cross & Naismith, 2014; Hail, Chen, & Bushman, 2010; Rudick & Sandrock, 2004). Considering these mechanisms of action, it is expectable for different treatments to promote a disbalance of the memory and naïve T lymphocytes pools in the periphery.

Table 7. Multiple linear regression models to predict CD8⁺ T lymphocytes subsets percentages using as dependent variables gender, age, MS progression form (RRMS and PPMS) and treatment.

		CD8⁺ T Lymphocytes		
		% Recent thymic emigrants	% Naïve	% Effector memory
Gender [a]	B	-3.746	-3.560	2.031
	SE	4.441	4.487	2.727
	β	-0.089	-0.085	0.075
	P	0.402	0.430	0.459
Age	B	-0.552	-0.495	0.231
	SE	0.186	0.188	0.114
	β	-0.375	-0.338	0.244
	P	**0.004**	**0.010**	**0.046**
RRMS [b]	B	9.273	8.115	5.137
	SE	7.480	7.558	4.593
	β	0.234	0.206	0.201
	P	0.219	0.286	0.267
PPMS [c]	B	-0.926	-2.465	10.356
	SE	6.547	6.616	4.020
	β	-0.019	-0.052	0.338
	P	0.888	0.710	**0.012**
Treatment [d]	B	-9.172	-8.097	5.362
	SE	6.769	6.840	4.156
	β	-0.232	-0.206	0.211
	P	0.179	0.240	0.201
F(5,76)		4.749	4.156	6.792
$R^2_{adjusted}$		0.188	0.163	0.263
P-value		**0.001**	**0.002**	**0.000**

[a] Reference category: female;
[b] Reference category: healthy individuals and PPMS patients;
[c] Reference category: healthy individuals and RRMS patients;
[d] Reference category: treatment naïve.

4.2.3. Effect of the Treatment on T Lymphocytes Subsets' Percentages

To determine how the different treatments relate to the differences observed on the percentage of cells, we decided to group the individuals in accordance their treatment regimen. Only RRMS individuals were on treatment, as available treatments have an almost null effect on PPMS patients and no licensed drugs are available for this form of progression (Feinstein, Freeman, & Lo, 2015). Patients enrolled in this study were on one of the following disease modified drug: natalizumab (n=23), fingolimod (n=4), or

teriflunomide (n=4) and IFN-β (1). As for IFN-β, because only one individual was on that treatment we decided to exclude him from this analysis (**Table 1.**).

The results obtained showed treatment-naïve RRMS patients were no different from healthy individuals in what concerns total, $CD4^+$ or $CD8^+$ T lymphocytes or their ratio (**Figure. 16**).

Regarding the contribution of each of the treatments on the total and on the $CD8^+$ T lymphocytes percentages, results showed that those were not affected by any of the immunomodulatory therapies (**Figure 16. A** and **C**). However, for individuals under fingolimod treatment, $CD4^+$ T lymphocytes percentages were significantly lower in comparison to healthy controls and treatment-naïve individuals (**Figure 16. B**), which reflected on a decrease of the $CD4^+$ to $CD8^+$ T lymphocytes ratio (**Figure 16. D**).

Among the $CD4^+$ T lymphocytes, RRMS patients under fingolimod treatment also presented lower RTEs and naïve T lymphocytes percentages in comparison to RRMS naïve individuals (**Figure 17. A** and **B**), as opposed to the higher percentages of EM $CD4^+$ T lymphocytes (**Figure 17. D**). The percentages of CM and T_{EMRA} $CD4^+$ T lymphocytes were not altered between the five groups (**Figure 17. E**). The alterations of the fingolimod-treated individuals on the naïve and memory subsets were reflected on a lower naïve to memory ratio on these individuals relatively to treatment-naïve RRMS patients (**Figure 17. F**).

About the $CD8^+$ T lymphocytes, the results showed a lower percentage of RTEs and naïve cells in individuals under fingolimod treatment in comparison to treatment-naïve RRMS patients (Figure 22. A and B). As for the $CD4^+$ T lymphocytes, the CM and T_{EMRA} subsets from the $CD8^+$ T lymphocytes seemed unaltered independently of the treatment (**Figure 18. C** and **E**). The EM $CD8^+$ T lymphocytes percentages were significantly augmented in individuals under natalizumab treatment in comparison to healthy controls (**Figure 18. D**) and, altogether these alterations were reflected on a lower naïve to memory $CD8^+$ T lymphocytes ratio on RRMS individuals under fingolimod treatment in comparison to treatment-naïve and healthy controls (**Figure 18. F**).

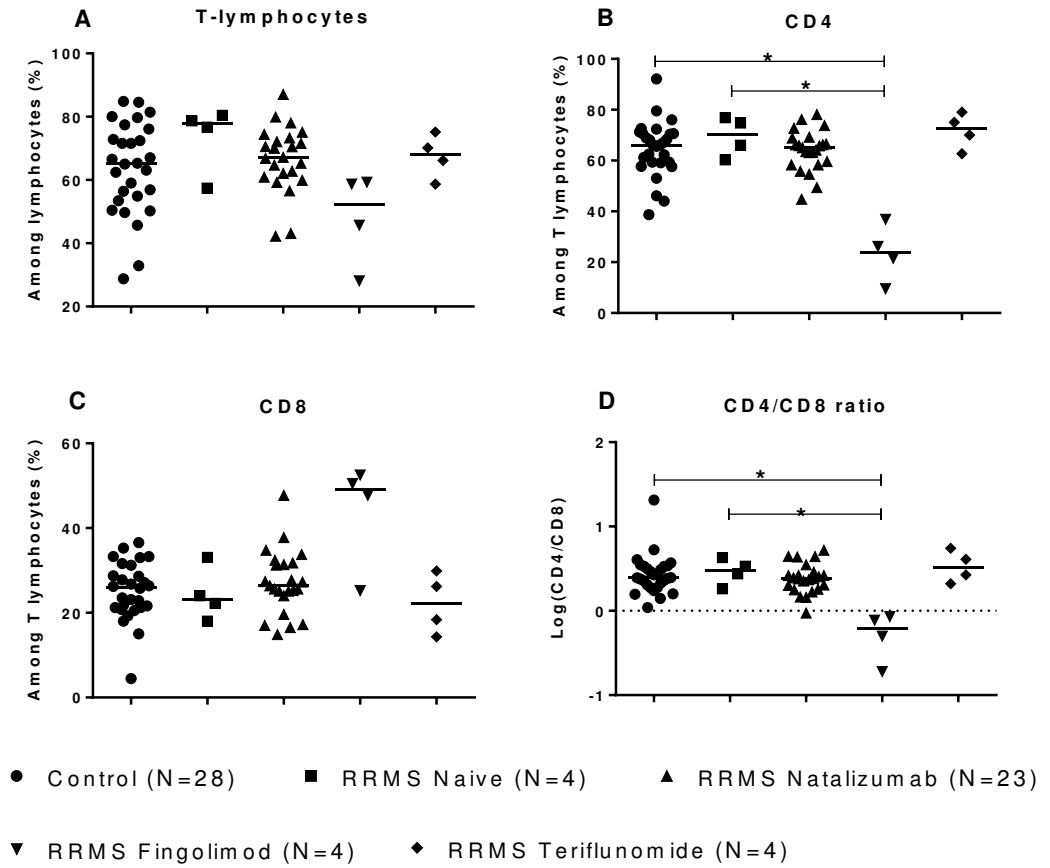

Figure 16. Effect of the immunomodulatory therapies on the percentage of T lymphocytes subsets. Represented are the total T lymphocytes [$\chi^2_{KW}(6,79)=8.187$, $p=0.1462$ (**A**)], $CD4^+$ T lymphocytes [$\chi^2_{KW}(6,79)=14.95$, $p=0.0106$ (**B**)], $CD8^+$ T lymphocytes [$\chi^2_{KW}(6,79)=8.794$, $p=0.1176$ (**C**)], and the $CD4^+$ to $CD8^+$ T lymphocytes ratio [$\chi^2_{KW}(6, 79)=14.64$, $p=0.0120$ (**D**)]. Each dot represents a single individual and the line the median of the group. Comparisons were performed using the non-parametric Kruskal-Wallis test followed by Dunn's multiple comparison tests; differences were considered statistically significant for p-value <0.05 and represented by * for $0.05>p>0.01$; ** $0.01\geq p>0.01$; and *** $0.001\geq p$; *N*, sample size.

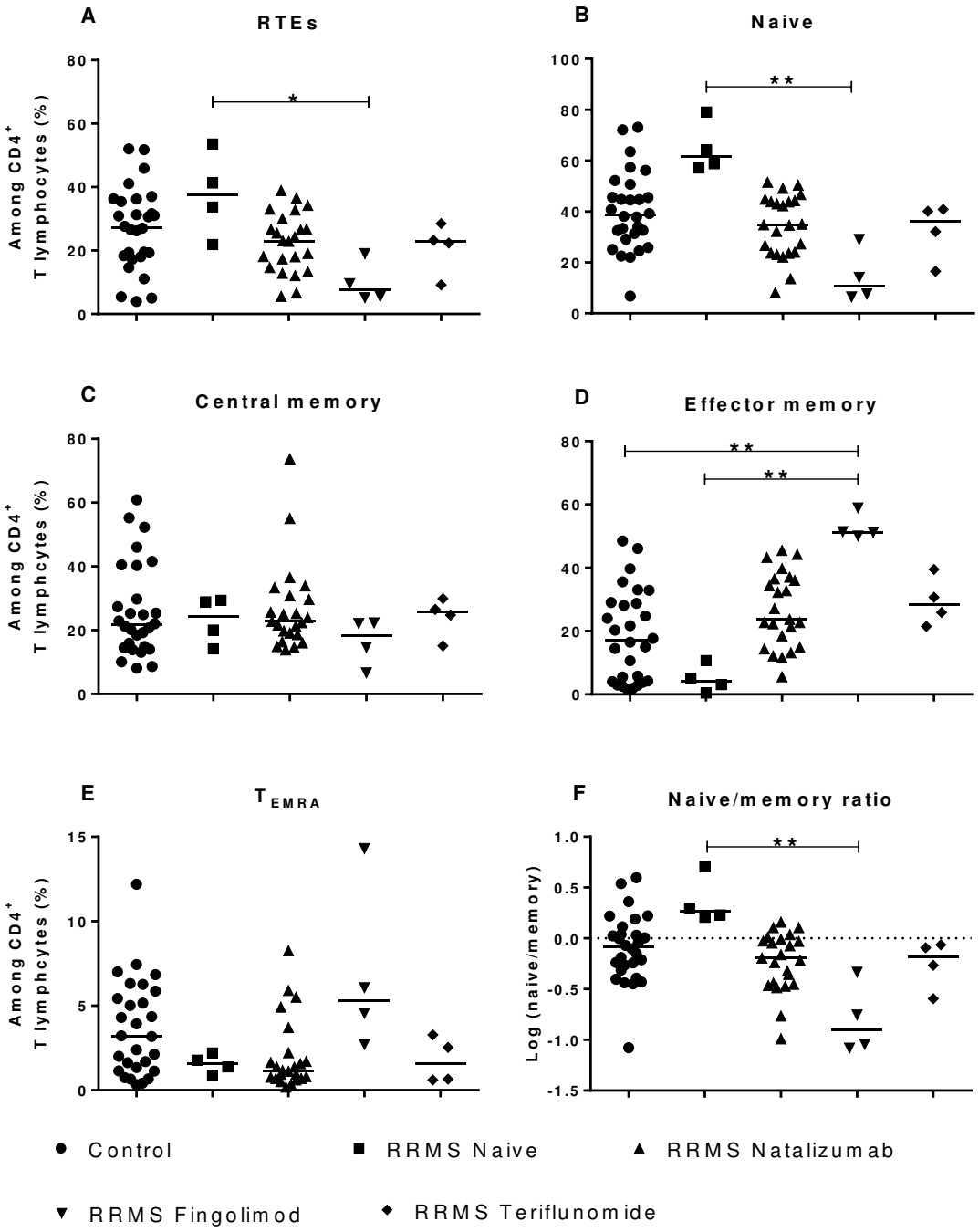

Figure 17. Effect of immunomodulatory therapies on the percentage of CD4⁺ T lymphocytes subsets. Represented are RTEs [$\chi^2_{KW}(6,79)=12.77$, $p=0.0257$ (**A**)], naïve [$\chi^2_{KW}(6,79)=17.61$, $p=0.0035$ (**B**)], central memory [CM; $\chi^2_{KW}(6,79)=5.428$, $p=0.3660$ (**C**)], effector memory [EM; $\chi^2_{KW}(6,79)=25.08$, $p=0.0001$ (**D**)], and T_{EMRA} [$\chi^2_{KW}(6,79)=11.45$, $p=0.0432$ (**E**)] CD4⁺ T lymphocytes. The naïve to memory ratio was calculated as the ratio of the naïve over the sum of CM, EM and T_{EMRA} subsets [$\chi^2_{KW}(6, 79)=18.06$, $p=0.0029$ (**F**)]. Each dot represents a single individual and the line the median of the group. Comparisons were performed using the non-parametric Kruskal-Wallis test followed by Dunn's multiple comparison tests; differences were considered statistically significant for *p*-value <0.05 and represented by * for 0.05>p>0.01; ** 0.01≥*p*>0.01; ** 0.001≥*p*; *N*, sample size.

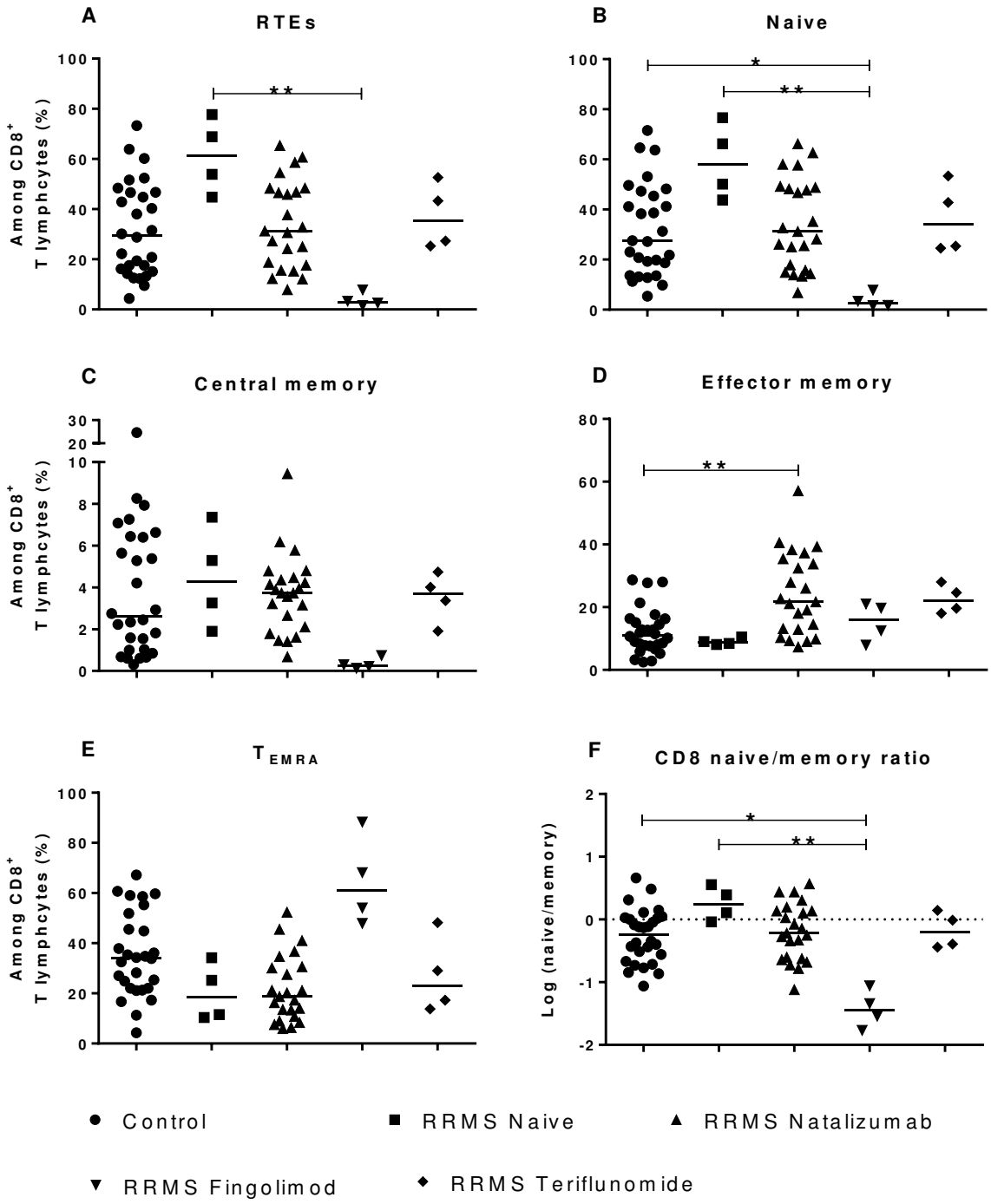

Figure 18. Effect of immunomodulatory therapies on the percentage of CD8⁺ T lymphocytes subsets. Represented are RTEs [$\chi^2_{KW}(6,79)=26.50$, $p<0.0001$ (**A**)], naïve [$\chi^2_{KW}(6,79)=27.62$, $p<0.0001$ (**B**)], central memory [CM; $\chi^2_{KW}(6,79)=13.09$, $p=0.0226$ (**C**)], effector memory [EM; $\chi^2_{KW}(6,79)=30.41$, $p=<0.0001$ (**D**)], and T_{EMRA} [$\chi^2_{KW}(6,79)=25.75$, $p<0.0001$ (**E**)] CD8⁺ T lymphocytes'. The naïve to memory ratio was calculated as the ratio of naïve over the sum of CM, EM ad T_{EMRA} subsets [$\chi^2_{KW}(6,79)=29.48$, $p<0.0001$ (**F**)]. Each dot represents a single individual. Comparisons were performed using the non-parametric Kruskal-Wallis test followed by Dunn's multiple comparisons test; differences were considered statistically significant for *p*-value <0.05 and represented by * for 0.05>p>0.01; ** 0.01≥*p*>0.01; ** 0.001≥*p*; *N*, sample size.

The results showed that most of the T lymphocytes subsets were altered in RRMS patients under fingolimod treatment. This observation is concordant to the mechanism of action pointed to this treatment as fingolimod leads to the sequestration of T lymphocytes within the lymphoid organs. The cell types most affected by this drug are the RTEs, naïve and the CM T lymphocytes as they present markers (e.g. CCR7 and CD62L) that promote their migration preferentially to these organs (V Brinkmann et al., 2010; Volker Brinkmann, 2009). Therefore, it is expected that under fingolimod treatment the number of CM and naïve T lymphocytes decrease on the periphery, which ultimately would contribute to increased percentage of EM T lymphocytes on the periphery in detriment of the other cell subsets. This also explains the decreased naïve to memory T lymphocytes ratio both in $CD4^+$ and $CD8^+$ T lymphocytes.

Patients treated with the monoclonal antibody natalizumab presented higher percentages of EM $CD8^+$ T lymphocytes in comparison to healthy individuals. This result may be related to the fact that this treatment hampers the entrance of immune cells to the CNS (Brown, 2009; Rudick & Sandrock, 2004) thus leading to the accumulation of these cells in the periphery.

Our results suggest that the apparent immune system aging and reduced thymic function that we observed before for the RRMS patients might be more related to the fact most of them were on immunomodulatory treatments and not due to the pathophysiological characteristic of the disease as pointed by others (Duszczyszyn et al., 2010; Hug et al., 2003). Interestinguely, to the date the data existing about immune system aging and thymic function on multiple sclerosis regards mainly one of the forms of progression of MS (Duszczyszyn et al., 2006, 2010; Haegert et al., 2011; Hug et al., 2003). In most of these studies, data regarding treatment is poorly provided which hampers comparisons with our data. Therefore, to further substantiate these findings increased thymic function and immune system aging surrogates' evaluation are necessary. Here, we provide analysis for both PPMS and RRMS.

On overall it will be imperative to increase the sample size. This will be particularly relevant to the comparisons between the RRMS treatment-naïve with the healthy controls and with the PPMS individuals as well as with the RRMS individuals under different therapies. The current sample size of fingolimod, teriflunomide and RRMS treatment naïve patients hampers essential comparisons that we aim to perform, namely, with the RRMS treated patients to determine if effectively the apparent thymic function

is lower in these individuals and the immune system aging is due to treatment and not a pathological characteristic of the disease. For that, we aim also to follow up the RRMS at treatment initiation and 6 months later.

So far we have determined the thymic function and the immune system aging by quantification of the cells exported from the thymus and establishment of the naïve over memory ratio, respectively. Although the contribution of these surrogates to address our question, we must consider that various factors may change these readouts, including the peripheral proliferation profile of these cells. Determination of cellular peripheral proliferation is imperative to substantiate our conclusions as quantification of RTEs based on the high expression of CD31 may be altered by thymic exportation of newly formed T lymphocytes, but can also be a result of high peripheral proliferation without any impairment of thymic function. To overcome this issue, we aim to quantify the sj/βTREC ratio as this surrogate of the thymic function is not affected by peripheral proliferation. We also aim to quantify the length of telomere repeats through the protocol already optimized in the laboratory in the context on this MSc thesis. The quantification of the former will provide us information about T lymphocytes aging since telomeres decrease as cells proliferate. The outcome provided by the quantification of the length of telomeres repeats, sj/βTREC ratio and peripheral proliferation will allow us to better determine immune system aging as well thymic funtion in patients with different MS progression forms and healthy controls.

5. CONCLUSION

With this study, we aimed to study how thymic function and immune system aging could be contributing to the development of the different forms of progression of multiple sclerosis. We hypothesized that the different forms of progression could present differences on the thymic function and immune system aging. Our results suggest that naïve and memory T lymphocytes subsets become unbalanced and that RTEs are altered with age in RRMS in comparison to healthy controls or PPMS individuals. As most of the RRMS individuals are under treatment our results suggest that the results observed for RTEs and naïve to memory ratio are most probably because of therapy and not as a cause/consequence of the MS progression form.

We hope this study contributes to the increase understanding of thymic function and immune system aging on the pathophysiological events that characterize the different forms of progression of MS and on the alterations induced by MS-treatment. This understanding might have high relevance because new strategies may be adopted and adapted to treat this disease.

6. REFERENCES

Akbar, A. N., & Vukmanovic-Stejic, M. (2007). Telomerase in T lymphocytes: use it and lose it? *Journal of Immunology*, *178*(11), 6689–6694.

Aktas, O., Küry, P., Kieseier, B., & Hartung, H. P. (2010). Fingolimod is a potential novel therapy for multiple sclerosis. *Nature Reviews Neurology*, *6*(7), 373–382.

Allsopp, R. C., Chang, E., Kashefi-Aazam, M., Rogaev, E. I., Piatyszec, M. A., Shay, J. W., & Harley, C. B. (1995). Telomere shortening is associated with cell division in vitro and in vivo. *Experimental Cell Research*, *220*, 194–200.

Antel, J., Antel, S., Caramanos, Z., Arnold, D. L., & Kuhlmann, T. (2012). Primary progressive multiple sclerosis: Part of the MS disease spectrum or separate disease entity? *Acta Neuropathologica*, *123*(5), 627–638.

Baerlocher, G. M., Vulto, I., de Jong, G., & Lansdorp, P. M. (2006). Flow cytometry and FISH to measure the average length of telomeres (flow FISH). *Nature Protocols*, *1*(5), 2365–2376.

Bains, I., Yates, A. J., & Callard, R. E. (2013). Heterogeneity in Thymic Emigrants: Implications for Thymectomy and Immunosenescence. *PLoS ONE*, *8*(2), 1–10.

Balint, B., Schwarz, A., Jarius, S., Engelhardt, K., Bussmann, C., Ebinger, F., ... Huppke, P. (2013). T-cell homeostasis in pediatric multiple sclerosis. *Neurology*, *81*(9), 784–792.

Beecham, A. H., Patsopoulos, N. A., Xifara, D. K., Davis, M. F., Kemppinen, A., Cotsapas, C., ... Goris, A. (2013). Analysis of immune-related loci identifies 48 new susceptibility variants for multiple sclerosis. *Nature Genetics*, *45*(11), 1353–60.

Benz, C., Heinzel, K., & Bleul, C. C. (2004). Homing of immature thymocytes to the subcapsular microenvironment within the thymus is not an absolute requirement for T cell development. *European Journal of Immunology*, *34*(12), 3652–3663.

Boehmer, H. von, & Melchers, F. (2010). Checkpoints in lymphocyte development and autoimmune disease. *Nature Immunology*, *11*(1), 14–20.

Briceño, O., Lissina, A., Wanke, K., Afonso, G., von Braun, A., Ragon, K., … Appay, V. (2016). Reduced naïve CD8+ T-cell priming efficacy in elderly adults. *Aging Cell*, *15*(1), 14–21.

Brinkmann, V. (2009). FTY720 (fingolimod) in Multiple Sclerosis: Therapeutic effects in the immune and the central nervous system. *British Journal of Pharmacology*, *158*(5), 1173–1182.

Brinkmann, V., Billich, A., Baumruker, T., Heining, P., Schmouder, R., Francis, G., … Burtin, P. (2010). Fingolimod (FTY720): discovery and development of an oral drug to treat multiple sclerosis. *Nature Reviews Drug Discovery*, *9*(11), 883–897.

Brown, B. A. (2009). Natalizumab in the treatment of multiple sclerosis. *Nature Clinical Practice Neurology*, *2*(2), 585–594.

Chaudhry, M. S., Dudakov, J. A., Brink, M. R. M. Van Den, & Brink, M. R. M. Van Den. (2016). Thymus : the next (re) generation. *Immunological Reviews*, *271*, 56–71.

Compston, A., & Coles, A. (2008). Multiple sclerosis. *The Lancet*, *372*, 1502–1517.

Correia, A. S., Augusto, L., Meireles, J., Pinto, J., & Sousa, A. P. (2016). Pediatric multiple sclerosis in Portugal: A multicentre study. *Acta Medica Portugal*, *29*(7–8), 425–431.

Cross, A. H., & Naismith, R. T. (2014). Established and novel disease-modifying treatments in multiple sclerosis. *Journal of Internal Medicine*, *275*(4), 350–363.

Demeure, C. E., Byun, D. G., Yang, L. P., Vezzio, N., & Delespesse, G. (1996). CD31 (PECAM-1) is a differentiation antigen lost during human CD4 T-cell maturation into Th1 or Th2 effector cells. *Immunology*, *88*, 110–115.

Dendrou, C. A., Fugger, L., & Friese, M. A. (2015). Immunopathology of multiple sclerosis. *Nature Reviews Immunology*, *15*(9), 545–558.

Dik, W. A., Pike-Overzet, K., Weerkamp, F., de Ridder, D., de Haas, E. F. E., Baert, M. R. M., ... Staal, F. J. T. (2005). New insights on human T cell development by quantitative T cell receptor gene rearrangement studies and gene expression profiling. *Journal of Experimental Medicine*, *201*(11), 1715–1723.

Dion, M. L., Poulin, J. F., Bordi, R., Sylvestre, M., Corsini, R., Kettaf, N., ... Cheynier, R. (2004). HIV infection rapidly induces and maintains a substantial suppression of thymocyte proliferation. *Immunity*, *21*(6), 757–768.

Dion, M., Sékaly, R., & Cheynier, R. (2007). Estimating thymic function through quantification of T-cell receptor excision circles. *Methods in Molecular Biology*, *380*(3), 197–213.

Duszczyszyn, D. A., Beck, J. D., Antel, J., Bar-Or, A., Lapierre, Y., Gadag, V., & Haegert, D. G. (2006). Altered naive CD4 and CD8 T cell homeostasis in patients with relapsing-remitting multiple sclerosis: Thymic versus peripheral (non-thymic) mechanisms. *Clinical and Experimental Immunology*, *143*(2), 305–313.

Duszczyszyn, D. A., Williams, J. L., Mason, H., Lapierre, Y., Antel, J., & Haegert, D. G. (2010). Thymic involution and proliferative T-cell responses in multiple sclerosis. *Journal of Neuroimmunology*, *221*(1–2), 73–80.

Ebers, G. C., Sadovnick, A. D., & Risch, & N. J. (1995). A genetic basis for familial aggregation in multiple sclerosis. *Nature*, *377*, 150–151.

Engelhardt, B., & Ransohoff, R. M. (2005). The ins and outs of T-lymphocyte trafficking to the CNS: Anatomical sites and molecular mechanisms. *Trends in Immunology*, *26*(9), 485–495.

Engelhardt, B., Vajkoczy, P., & Weller, R. O. (2017). The movers and shapers in immune privilege of the CNS. *Nature Immunology*, 18, 123-131.

Farber, D. L., Yudanin, N. a, & Restifo, N. P. (2013). Human memory T cells: generation, compartmentalization and homeostasis. *Nature Reviews Immunology*, *14*(1), 24–35.

Farh, K. K.-H., Marson, A., Zhu, J., Kleinewietfeld, M., Housley, W. J., Beik, S., ... Bernstein, B. E. (2014). Genetic and epigenetic fine mapping of causal autoimmune disease variants. *Nature*, *518*, 337–43.

Feinstein, A., Freeman, J., & Lo, A. C. (2015). Treatment of progressive multiple sclerosis: What works, what does not, and what is needed. *Lancet Neurology*, *14*(2), 194–207.

Figueiredo, J., Silva, A., Cerqueira, J. J., Fonseca, J., & Pereira, P. A. (2015). MS prevalence and patients' characteristics in the district of braga, Portugal. *Neurology Research International*, DOI: 10.1155/2015/895163

Filippi, M., Rocca, M. A., Ciccarelli, O., De Stefano, N., Evangelou, N., Kappos, L., ... Barkhof, F. (2016). MRI criteria for the diagnosis of multiple sclerosis: MAGNIMS consensus guidelines. *Lancet Neurology*, *15*, 292–303.

Fink, P. J. (2012). The biology of recent thymic emigrants. *Annual Review of Immunology*, *31*, 31–50.

Fletcher, J. M., Lalor, S. J., Sweeney, C. M., Tubridy, N., & Mills, K. H. G. (2010). T cells in multiple sclerosis and experimental autoimmune encephalomyelitis. *Clinical and Experimental Immunology*, *162*(1), 1–11.

Förster, R., Schubel, A., Breitfeld, D., Kremmer, E., Renner-Müller, I., Wolf, E., & Lipp, M. (1999). CCR7 coordinates the primary immune response by establishing functional microenvironments in secondary lymphoid organs. *Cell*, *99*(1), 23–33.

Gameiro, J., Nagib, P., & Verinaud, L. (2010). The thymus microenvironment in regulating thymocyte differentiation. *Cell Adhesion and Migration*, *4*(3), 382–390.

Geenen, V., Poulin, J. F., Dion, M. L., Martens, H., Castermans, E., Hansenne, I., ... Cheynier, R. (2003). Quantification of T cell receptor rearrangement of excision circles to estimate thymic function: An important new tool for endocrine-immune physiology. *Journal of Endocrinology*, *176*, 305–311.

Geiger, H., & Rudolph, K. L. (2009). Aging in the lympho-hematopoietic stem cell compartment. *Trends in Immunology*, *30*(7), 360–365.

Georgin-Lavialle, S., Aouba, A., Mouthon, L., Londono-Vallejo, J. A., Lepelletier, Y., Gabet, A. S., & Hermine, O. (2010). The telomere/telomerase system in autoimmune and systemic immune-mediated diseases. *Autoimmunity Reviews*, *9*(10), 646–651.

Germain, R. N. (2002). T-cell development and the CD4-CD8 lineage decision. *Nature Reviews Immunology*, *2*(5), 309–322.

Gonsette, R. E. (2012). Self-tolerance in multiple sclerosis. *Acta Neurologica Belgica*, *112*(2), 133–140.

Grigoriadis, N., & Pesch, V. van. (2015). A basic overview of multiple sclerosis immunopathology. *European Journal of Neurology*, *22*, 3–13.

Gui, J., Mustachio, L. M., Su, D.-M., & Craig, R. W. (2012). Thymus Size and Age-related Thymic Involution: Early Programming, Sexual Dimorphism, Progenitors and Stroma. *Aging and Disease*, *3*(3), 280–90.

Haegert, D. G., Hackenbroch, J. D., Duszczyszyn, D., Fitz-Gerald, L., Zastepa, E., Mason, H., ... Bar-Or, A. (2011). Reduced thymic output and peripheral naïve CD4 T-cell alterations in primary progressive multiple sclerosis (PPMS). *Journal of Neuroimmunology*, *233*, 233–239.

Hail, N., Chen, P., & Bushman, L. R. (2010). Teriflunomide (leflunomide) promotes cytostatic, antioxidant, and apoptotic effects in transformed prostate epithelial cells: evidence supporting a role for teriflunomide in prostate cancer chemoprevention. *Neoplasia*, *12*(6), 464–475.

Hartmann, F. J., Khademi, M., Aram, J., Ammann, S., Kockum, I., Constantinescu, C., ... Becher, B. (2014). Multiple sclerosis-associated IL2RA polymorphism controls GM-CSF production in human TH cells. *Nature Communications*, *5*, 5056.

Hazenberg, M. D., Verschuren, M. C., Hamann, D., Miedema, F., & Dongen, J. J. (2001). T cell receptor excision circles as markers for recent thymic emigrants: Basic aspects, technical approach, and guidelines for interpretation. *Journal of Molecular Medicine*, *79*(11), 631–640.

Hemmer, B., Kerschensteiner, M., & Korn, T. (2015). Role of the innate and adaptive immune responses in the course of multiple sclerosis. *The Lancet Neurology*, *14*(4), 406–419.

Hoppenbrouwers, I. A., & Hintzen, R. Q. (2011). Genetics of multiple sclerosis. *Biochimica et Biophysica*, *Acta 1812*, 194–201.

Horta, A., Nobrega, C., Amorim-Machado, P., Coutinho-Teixeira, V., Barreira-Silva, P., Boavida, S., ... Correia-Neves, M. (2013). Poor Immune Reconstitution in HIV-Infected Patients Associates with High Percentage of Regulatory CD4+ T Cells. *PLoS ONE*, *8*(2), 1–7.

Hug, A., Korporal, M., Schroder, I., Haas, J., Glatz, K., Storch-Hagenlocher, B., & Wildemann, B. (2003). Thymic Export Function and T Cell Homeostasis in Patients with Relapsing Remitting Multiple Sclerosis. *The Journal of Immunology*, *171*(1), 432–437.

Johannisson, A., & Festin, R. (1995). Phenotype transition of CD4+ T cells from CD45RA to CD45R0 is accompanied by cell activation and proliferation. *Cytometry*, *19*(4), 343–52.

Junge, S., Kloeckener-Gruissem, B., Zufferey, R., Keisker, A., Salgo, B., Fauchere, J. C., ... Gungor, T. (2007). Correlation between recent thymic emigrants and CD31+ (PECAM-1) CD4+ T cells in normal individuals during aging and in lymphopenic children. *European Journal of Immunology*, *37*(11), 3270–3280.

Khoury, S. J., Guttmann, C. R., Orav, E. J., Kikinis, R., Jolesz, F. a, & Weiner, H. L. (2000). Changes in activated T cells in the blood correlate with disease activity in multiple sclerosis. *Archives of Neurology*, *57*(8), 1183–9.

Klein, L., Hinterberger, M., Wirnsberger, G., & Kyewski, B. (2009). Antigen presentation in the thymus for positive selection and central tolerance induction. *Nature Reviews. Immunology*, *9*(12), 833–844.

Klein, L., Kyewski, B., Allen, P. M., & Hogquist, K. (2014). Positive and negative selection of the T cell repertoire: what thymocytes see (and don't see). *Nature Reviews Immunology*, *14*(6), 377–91.

Kumar, D. R., Aslinia, F., Yale, S. H., & Mazza, J. J. (2011). Jean-Martin Charcot: The Father of Neurology. *Clinical Medicine and Research*, *9*(1), 46–49.

Kwan, J., & Killeen, N. (2004). CCR7 directs the migration of thymocytes into the thymic medulla. *Journal of Immunology*, *172*(7), 3999–4007.

Ladi, E., Yin, X., Chtanova, T., & Robey, E. a. (2006). Thymic microenvironments for T cell differentiation and selection. *Nature Immunology*, *7*(4), 338–343.

Linton, P. J., & Dorshkind, K. (2004). Age-related changes in lymphocyte development and function. *Nature Reviews Immunology*, *5*(2), 133–139.

Lublin, F. D., Reingold, S. C., Cohen, J. A., Cutter, G. R., Thompson, A. J., Wolinsky, J. S., ... Lubetzki, C. (2014). Defining the clinical course of multiple sclerosis : The 2013 revisions. *Neurology*, *83*, 278–286.

Lublin, F. D., Reingold, S. C., & Tiqwa, P. (1996). Defining the clinical course of multiple sclerosis: Results of an international survey. *Neurology*, *46*, 907–911.

Lundström, W., Highfill, S., Walsh, S. T. R., Beq, S., Morse, E., Kockum, I., ... Mackall, C. L. (2013). Soluble IL7Rα potentiates IL-7 bioactivity and promotes autoimmunity. *Proceedings of the National Academy of Sciences of the United States of America*, *110*(19), E1761-70.

Lynch, H. E., Goldberg, G. L., Chidgey, A., Van den Brink, M. R. M., Boyd, R., & Sempowski, G. D. (2009). Thymic involution and immune reconstitution. *Trends in Immunology*, *30*(7), 366–373.

Mahnke, Y. D., Brodie, T. M., Sallusto, F., Roederer, M., & Lugli, E. (2013). The who's who of T-cell differentiation: Human memory T-cell subsets. *European Journal of Immunology*, *43*(11), 2797–2809.

Maus, M. V, Kovacs, B., Kwok, W. W., Nepom, G. T., Schlienger, K., Riley, J. L., ... June, C. H. (2004). Extensive replicative capacity of human central memory T cells. *Journal of Immunology*, *172*(11), 6675–6683.

McMahon, E. J., Bailey, S. L., Castenada, C. V., Waldner, H., & Miller, S. D. (2005). Epitope spreading initiates in the CNS in two mouse models of multiple sclerosis. *Nature Medicine*, *11*(3), 335–339.

Multiple Sclerosis International Federation (2013). *Atlas of MS 2013*. Retrieved from https://www.msif.org/wp-content/uploads/2014/09/Atlas-of-MS.pdf

Minagar, A., & Alexander, J. S. (2003). Blood-brain barrier disruption in multiple sclerosis, *Multiple Sclerosis*, 9(6), 540–549.

Misslitz, A., Pabst, O., Hintzen, G., Ohl, L., Kremmer, E., Petrie, H. T., & Förster, R. (2004). Thymic T cell development and progenitor localization depend on CCR7. *The Journal of Experimental Medicine*, *200*(4), 481–491.

Montpetit, A. J., Alhareeri, A. A., Montpetit, M., Starkweather, A. R., Elmore, L. W., Filler, K., ... Jackson-Cook, C. K. (2014). Telomere length a review of methods for measurement. *Nursing Research*, *63*(4), 289–299.

Murray, T. J. (2009). The history of multiple sclerosis: the changing frame of the disease over the centuries. *Journal of the Neurological Sciences*, *277*(SUPPL. 1), S3–S8.

Naylor, K., Li, G., Vallejo, A. N., Lee, W.-W., Koetz, K., Bryl, E., ... Goronzy, J. J. (2005). The influence of age on T cell generation and TCR diversity. *Journal of Immunology (Baltimore, Md. : 1950)*, *174*(11), 7446–7452. http://doi.org/10.4049/jimmunol.174.11.7446

Nobrega, C., Horta, A., Coutinho-Teixeira, V., Martins-Ribeiro, A., Baldaia, A., Rb-Silva, R., ... Correia-Neves, M. (2016). Longitudinal evaluation of regulatory T cells dynamics on HIV-infected individuals during the first two years of therapy. *AIDS*, *30*, 1175–1185.

Nunes-Cabaço, H., & Sousa, A. E. (2013). Repairing thymic function. *Current Opinion in Organ Transplantation*, *18*, 363–368.

Olson, J. K., & Miller, S. D. (2004). Microglia initiate central nervous system innate and adaptive immune responses through multiple TLRs. *The Journal of Immunology*, *173*(6), 3916–3924.

Olsson, T., Barcellos, L. F., & Alfredsson, L. (2016). Interactions between genetic, lifestyle and environmental risk factors for multiple sclerosis. *Nature Reviews Neurology*. 13, 25-36.

Pearce, J. M. S. (2005). Historical descriptions of multiple sclerosis. *European Neurology*, *54*(1), 49–53.

Pido-Lopez, J., Imami, N., & Aspinall, R. (2001). Both age and gender affect thymic output: More recent thymic migrants in females than males as they age. *Clinical and Experimental Immunology*, *125*(3), 409–413.

Pinto, L., Covas, M. J., & Victorino, R. M. (1991). Loss of CD45RA and gain of CD45RO after in vitro activation of lymphocytes from HIV-infected patients. *Immunology*, *73*(2), 147–50.

Polman, C. H., Reingold, S. C., Banwell, B., Clanet, M., Cohen, J. A., Filippi, M., ... Wolinsky, J. S. (2011). Diagnostic criteria for multiple sclerosis: 2010 revisions to the McDonald criteria. *Annals of Neurology*, *69*, 292–302.

Poulin, J., Sylvestre, M., Champagne, P., Dion, M., Kettaf, N., Lainesse, M., ... Dc, W. (2012). Evidence for adequate thymic function but impaired naive T-cell survival following allogeneic hematopoietic stem cell transplantation in the absence of chronic graft-versus-host disease Evidence for adequate thymic function but impaired naive T-cell survi. *Blood*, *102*(13), 4600–4607.

Prockop, S. E., & Petrie, H. T. (2004). Regulation of thymus size by competition for stromal niches among early T cell progenitors. *Journal of Immunology*, *173*, 1604–1611.

Reboul, J., Mertens, C., Levillayer, F., Eichenbaum-Voline, S., Vilkoren, T., Cournu, I., ... Liblau, R. (2000). Cytokines in genetic susceptibility to multiple sclerosis: A candidate gene approach. *Journal of Neuroimmunology*, *102*(1), 107–112.

Richards, D. M., Kyewski, B., & Feuerer, M. (2016). Re-examining the nature and function of self-reactive T cells. *Trends in Immunology*, *37*(2), 114–125.

Rossi, F. M. V, Corbel, S. Y., Merzaban, J. S., Carlow, D. a, Gossens, K., Duenas, J., ... Ziltener, H. J. (2005). Recruitment of adult thymic progenitors is regulated by P-selectin and its ligand PSGL-1. *Nature Immunology*, *6*(6), 626–634.

Rudick, R. A., & Sandrock, A. (2004). Natalizumab: [alpha]4-integrin antagonist selective adhesion molecule inhibitors for MS. *Expert Review of Neurotherapeutics*, *4*(4), 571–80.

Sadovnick, A. D., Armstrong, H., Rice, G. P. A., Bulman, D., Hashimoto, L., Paty, D. W., ... Weinshenker, B., Brunet D., (1993). A Population-Based Study of Multiple Sclerosis in Twins. *Annals of Neurology*, *33*, 281–285.

Sallusto, F., Lenig, D., Förster, R., Lipp, M., & Lanzavecchia, A. (1999). Two subsets of memory T lymphocytes with distinct homing potentials and effector functions. *Nature*, *401*(6754), 708–712.

Saule, P., Trauet, J., Dutriez, V., Lekeux, V., Dessaint, J. P., & Labalette, M. (2006). Accumulation of memory T cells from childhood to old age: Central and effector memory cells in CD4+ versus effector memory and terminally differentiated memory cells in CD8+ compartment. *Mechanisms of Ageing and Development*, *127*(3), 274–281.

Serana, F., Chiarini, M., Zanotti, C., Sottini, A., Bertoli, D., Bosio, A., ... Imberti, L. (2013). Use of V (D) J recombination excision circles to identify T- and B-cell defects and to monitor the treatment in primary and acquired immunodeficiencies, *Journal of Translational Medicine*, 11, 111–119.

Shechter, R., London, A., & Schwartz, M. (2013). Orchestrated leukocyte recruitment to immune-privileged sites: absolute barriers versus educational gates. *Nature Reviews Immunology*, *13*(3), 206–218.

Sprent, J., & Surh, C. (2011). Normal T cell homeostasis: the conversion of naïve cells into memory-phenotype cells. *Nature Immunology*, *12*(6), 478–484.

Stinissen, P., & Hellings, N. (2008). Activation of myelin reactive T cells in multiple sclerosis: A possible role for T cell degeneracy? *European Journal of Immunology*, *38*(5), 1190–1193.

Takahama, Y. (2006). Journey through the thymus: stromal guides for T-cell development and selection. *Nature Reviews Immunology*, *6*(2), 127–35.

Tutuncu, M., Tang, J., Zeid, N. A., Kale, N., Crusan, D. J., Atkinson, E. J., ... Kantarci, O. H. (2013). Onset of progressive phase is an age-dependent clinical milestone in multiple sclerosis. *Multiple Sclerosis, 19*(2), 188–98.

Vargas-Lowy, D., & Chitnis, T. (2012). Pathogenesis of Pediatric Multiple Sclerosis. *Journal of Child Neurology*, *27*(11), 1394–1407.

Weber, F., Fontaine, B., Cournu-Rebeix, I., Kroner, A., Knop, M., Lutz, S., ... Muller-Myhsok, B. (2008). IL2RA and IL7RA genes confer susceptibility for multiple sclerosis in two independent European populations. *Genes Immunology*, *9*(3), 259–263.

Young, I. R., Hall, A. S., Pallis, C. A., Legg, N. J., Bydder, G. M., & Steiner, R. E. (1981). Nuclear magnetic resonance imaging of the brain in multiple sclerosis. *Lancet*. 2(8255), 1063-6.